

Performance of Diversity Techniques at Mobile Handset in Fading Channels

A Thesis

Submitted towards the partial fulfillment for the requirements for the award of the degree of

Master of Engineering

In

Electronics and Communication

by

Shivali Goel

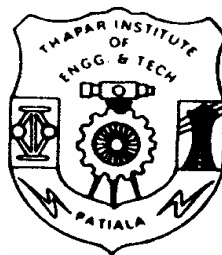
Regn. No. 8024123

Under the guidance of

Mr. R. Khanna

Assistant Professor

Department of Electronics & Communication Engineering



Department of Electronics & Communication Engineering

THAPAR INSTITUTE OF ENGINEERING AND TECHNOLOGY

(Deemed University)

Patiala-147004

June-2004

Certificate

This is to certify that the thesis entitled “*Performance of Diversity Techniques at Mobile Handset in Fading Channel*” submitted by Shivali Goel, Regn. No. 8024123, in partial fulfillment for the requirements for the award of Degree of Masters of Technology, to Thapar Institute of Engineering and Technology (Deemed University), Patiala, is a record of student’s own work carried out by her under my supervision and guidance. The report has not been submitted for the award of any other degree or certificate in this or any other university or institute.

(Mr. R. Khanna)

SUPERVISOR
Electronics & Communication Engineering Department
Thapar Institute of Engg. & Tech.
Patiala

Countersigned By:

(Dr. R. S. Kaler)
HEAD
Electronics & Communication Engg. Deptt.
Thapar institute of Engg. & Tech.
Patiala

(Dr. D.S. Bawa)
DEAN (Academic Affairs)
Thapar Institute of Engg. & Tech.
Patiala

Acknowledgement

I thank the almighty whose blessings have enabled me to accomplish my dissertation work successfully.

It is my pride privilege to express my sincere thanks and deep sense of gratitude to **Mr. R. Khanna**, Assistant Professor, Electronics and Communication Engineering Department, for his valuable advice, splendid supervision and constant patience through which this work was able to take the shape in which it has been presented. It was his valuable discussions and endless endeavors through which I have gained a lot. His constant encouragement and confidence-imbibing attitude has always been a moral support for me.

My sincere thanks to **Dr. R. S. Kaler**, Head, Electronics and Communication Engineering Department, for his immense concern throughout the project work.

A special word of thanks to all the faculty members for their constant encouragement, valuable, critical & timely suggestions; discussions and support throughout the duration.

I feel to express my most heartfelt and cordial thanks to my friends for giving me moral support and fortitude during critical times. I wish to extend a warm thanks to everybody who could not find a separate name but have helped directly or indirectly with my work.

Lastly but above all, I would like to mention that the whole credit of my achievements goes to my parents and family. They bestowed upon me the love & affection, which has been a constant source of inspiration. It was their unshakable faith in me that has kept me going.

Date:

(Shivali Goel)

Abstract

The demands for greater capacity and lower transmitted power have historically motivated research in spatial diversity systems. Diversity techniques have been implemented in many current systems and have been shown to reduce the transmit power required to maintain acceptable system performance. Traditionally spatial diversity is based on the transmission and reception of a single stream of symbols through independent and spatially separated propagation channels. In more recent developments, new techniques use diversity concepts to resolve multiple independent streams of data and increase the potential data-rate. The effectiveness of these multi-element arrays in communication systems has been found to depend on antenna design and specific characteristics of the propagation channels.

In this thesis, we derive bit error performance bounds for various statistical and spatial channel models with diversity combining. Statistical Channel models include the Rayleigh Fading, Ricean Fading, and Nakagami Fading Channel. The spatial channel models include the Geometrical Based Single Bounce (GBSB) Circular and Elliptical Channel models. The simulation of statistical channels shows that the probability of error decreases as the SNR increase. The BER also improves by applying various diversity techniques and among the three diversity combining techniques applied viz. maximal ratio combining (MRC), equal gain combining (EGC), and selection combining (SC), MRC shows the best performance. The performance of the antenna system also improves as the number of antenna elements is increased.

The spatio-temporal channel models provide a statistical description of the multipath channel parameters such as channel gain, propagation delays, angle of arrivals (AOA) etc. However, for the purpose of analysis, a simple parametric model represented by a summation of delta functions associated with different amplitudes, time delays and AOA is more useful. The channel coefficients are calculated first and then run the simulations to gather performance statistics of various micro diversity techniques like the MRC, EGC, and SC. Then the BER of various channels obtained as a result of simulation work for different diversity techniques and with varying number of antenna elements is compared. Results indicate that the MRC gives the best performance, EGC scheme performs close to MRC scheme and SC shows the poorest performance of all.

Table of Contents

Certificate	i
Acknowledgement	ii
Abstract	iii
Table of contents	iv-vi
List of Abbreviations	vii
List of Figures	viii-ix
List of Tables	x
Chapter 1 Introduction	1-5
1.1 Overview	1
1.2 Objectives of the thesis	4
1.3 Organization of thesis	5
Chapter 2 Multiple Antennas at Handsets	6-13
2.1 Introduction	6
2.2 Smart Antennas	6
2.3 Need of Adaptive Antennas at Handsets	7
2.4 Diversity techniques ate Handsets	8
2.5 Diversity Combining Techniques	9
2.6 Statistical Channel Models	10
2.7 Spatial Channel Models	12
Chapter 3 Diversity Techniques	14-24
3.1 Introduction	14
3.2 Diversity Techniques	14
3.3 Types of Diversity	15
3.3.1 Macroscopic diversity scheme	15
3.3.1 Microscopic diversity scheme	15
3.4 Basic Diversity Combining Methods	18
3.4.1 Selection diversity	18
3.4.2 Maximal ratio Combining	20
3.4.3 Equal Gain Combining	22
Chapter 4 Statistical Channel Models	25-59
4.1 Introduction	25

4.2	Small Scale Fading	26
4.3	Types of Small Scale Fading	27
4.3.1	Fast Fading	27
4.3.2	Slow Fading	28
4.3.3	Frequency Selective Fading	28
4.3.4	Flat Fading	28
4.4	Flat Fading Channel Models	29
4.4.1	Rayleigh Fading Channel	29
4.4.2	Ricean Fading Channel	30
4.4.3	Nakagami Fading Channel	32
4.5	Diversity Techniques in Statistical Fading Channel Models	32
4.6.1	Simulation of Diversity Techniques	33
4.6	Results and Discussion	35
Chapter 5	Spatial Channel Models	60-84
5.1	Overview	60
5.2	Multipath Propagation Environment	60
5.3	Advantages and disadvantages of GBSB models	63
5.3.1	Disadvantages	63
5.3.2	Advantages	63
5.4	GBSB Elliptical Model	63
5.4.1	Assumptions	64
5.4.2	Geometry and Notation	64
5.4.3	Mathematical Formulation	65
5.4.4	Generation of Samples of the Elliptical Channel Model	66
5.5	GBSB Circular Model	68
5.5.1	Assumptions	68
5.5.2	Geometry and Notation	69
5.5.3	Mathematical Formulation	70
5.5.4	Generation of Samples of the Circular Channel Model	70
5.6	Channel Description	71
5.7	Diversity Techniques in Spatial Channel Models	73
5.8	Results and Discussion	73

List of Abbreviations

AOA	Angle of Arrival
BER	Bit Error Rate
CDMA	Code Division Multiple Access
CIR	Carrier to Interference Ratio
<i>DCA</i>	<i>Dynamic Channel Assignment</i>
DOA	Direction of Arrival
DS-CDMA	Direct Sequence Code Division Multiple Access
EGC	Equal Gain Combiner
EIRP	Equivalent Isotropic Radiated Power
FDD	Frequency Division Duplex
FDMA	Frequency Division Multiple Access
GBSB	Geometrically Based Single Bounce
ISI	Intersymbol Interference
LOS	Line of Sight
MRC	Maximal Ratio Combiner
PCS	Personal Communication Services
QHA	Quadrifilar Helix Antenna
QoS	Quality of Service
RF	Radio Frequency
SC	Selective Combiner
SINR	Signal to Interference Plus Noise Ratio
SNR	Signal to Noise Ratio
TDMA	Time Division Multiple Access

List of Figures

Fig. No.	Title of Figure	Page No.
3.1	Selection Diversity	18
3.2	Probability for different values of M-Selection Combiner	20
3.3	Maximal Ratio Combining	20
3.4	Probability for different values of Maximal Ratio Combiner	21
3.5	Equal Gain Combining	22
3.6	Probability for M=2 Equal Gain Combiner	23
3.7	Performance Comparison Improvement of various Combining Techniques	24
4.1	Multipath Propagation of a Signal	27
4.2	Illustration of Rayleigh Fade Effect on a Signal	29
4.3	Plot of the Bit Error Probability vs. SNR for AWGN and Rayleigh Fading Channel	44
4.4	Plot of BER vs. Eb/No for 1-path Rayleigh Fading Channel	45
4.5	Plot of BER vs. Eb/No for Rayleigh Fading Channel using Second Order Diversity Combining Schemes	46
4.6	Plot of BER vs. Eb/No for 1-path Ricean Fading Channel	47
4.7	Plot of BER vs. Eb/No for Ricean Fading Channel using Second Order Diversity Combining Schemes	48
4.8	Plot of BER vs. Eb/No for 1-path Nakagami Fading Channel	49
4.9	Plot of BER vs. Eb/No for Nakagami Fading Channel using Second Order Diversity Combining Schemes	50
4.10	Plot of BER vs. Eb/No for Rayleigh Fading Channel with the increase in no. of antenna elements using EGC	51
4.11	Plot of BER vs. Eb/No for Rayleigh Fading Channel with the increase in no. of antenna elements using SC	52
4.12	Plot of BER vs. Eb/No for Rayleigh Fading Channel with the increase in no. of antenna elements using MRC	53
4.13	Plot of BER vs. Eb/No for Ricean Fading Channel with the increase in the no. of antenna elements using EGC	54
4.14	Plot of BER vs. Eb/No for Ricean Fading Channel with the increase in the no. of antenna elements using SC	55

4.15	Plot of BER vs. Eb/No for Ricean Fading Channel with the increase in the no. of antenna elements using MRC	56
4.16	Plot of BER vs. Eb/No for Nakagami Fading Channel with the increase in the no. of antenna elements using EGC	57
4.17	Plot of BER vs. Eb/No for Nakagami Fading Channel with the increase in the no. of antenna elements using SC	58
4.18	Plot of BER vs. Eb/No for Nakagami Fading Channel with the increase in the no. of antenna elements using MRC	59
5.1	The Simplified Multipath Environment	61
5.2	Geometry of the GBSB Elliptical Channel Model	64
5.3	Geometry of the Circular Scattering Channel Model	69
5.4	Plot of BER vs. Eb/No for 1-path GBSB Elliptical Channel	77
5.5	Plot of BER vs. Eb/No for 1-path GBSB Circular Channel	78
5.6	Plot of BER vs. Eb/No for GBSB Elliptical Channel with the increase in the no. of antenna elements using EGC	79
5.7	Plot of BER vs. Eb/No for GBSB Elliptical Channel with the increase in the no. of antenna elements using SC	80
5.8	Plot of BER vs. Eb/No for GBSB Elliptical Channel with the increase in the no. of antenna elements using MRC	81
5.9	Plot of BER vs. Eb/No for GBSB Circular Channel with the increase in the no. of antenna elements using EGC	82
5.10	Plot of BER vs. Eb/No for GBSB Circular Channel with the increase in the no. of antenna elements using SMC	83
5.11	Plot of BER vs. Eb/No for GBSB Circular Channel with the increase in the no. of antenna elements using MRC	84

List of Tables

Table No.	Title of Table	Page No.
4.1	Comparison of BER for 1-path and 2-order diversity combiner Rayleigh Fading Channel	39
4.2	Comparison of BER for 1-path and 2-order diversity combiner Ricean Fading Channel	39
4.3	Comparison of BER for 1-path and 2-order diversity combiner Ricean Fading Channel	40
4.4	Comparison of BER for diversity combiner Rayleigh Fading Channel for different no. of antenna elements	41
4.5	Comparison of BER for diversity combiner Ricean Fading Channel for different no. of antenna elements	42
4.6	Comparison of BER for diversity combiner Ricean Fading Channel or different no. of antenna elements	43
5.1	Comparison of BER for GBSB Elliptical Channel for different no. of antenna elements	75
5.2	Comparison of BER for GBSB Circular Channel for different no. of antenna elements	76

Chapter-1

Introduction

1.1 Overview

The wireless industry is witnessing an explosive growth today in the new millennium. The new generation wireless systems are being designed to provide ubiquitous broadband link access to information infrastructure. As the broadband wireless industry struggles to find the right technology to give operators what they need to provide service cost-effectively, smart antennas have entered the perspective of many as a very promising solution. With operators and manufacturers preparing and deploying Third Generation systems the increasing growth of mobile phone users has created a need for higher capacity & broadband cellular network. Even as more spectrum is allocated, demand for higher data rate services and steadily increasing numbers of users will motivate service providers to seek ways of increasing the capacity and bandwidth of their systems. One way of overcoming the problem is by using adaptive antennas on the handset.

Smart or adaptive antenna arrays can improve the performance of wireless communication systems [1]. Smart antennas can increase the coverage and capacity of a system. In multipath channels they can increase the maximum data rate and mitigate fading due to cancellation of multipath components. Adaptive antennas can also be used for direction finding, with applications including emergency services and vehicular traffic monitoring. By using an antenna system, one with more than one antenna port in the handset, it is possible to combine the signals from the antennas in such a way that both the Signal to Noise (SNR) level and the Carrier to Interference (CIR) level is improved. The power consumption at the handset can be lowered.

Unlike conventional cellular antennas, which broadcast energy over the entire cell, adaptive antennas confine the broadcast energy to a narrow beam. It optimizes the way that signals are distributed through space on a real time basis by focusing the signal to the desired user and “steering” it away from other users occupying the same channel in the same cell and adjacent or distant cell. Conventional antennas had to face several problems in wireless communications; a few of them includes

- Poor BER due to the range, which causes path loss.
- Poor BER due to uniformity of coverage, which causes fading.
- Poor BER due to Frequency reuse which causes co-channel interference.

- Need more capacity (reuse would affect the BER), which causes co-channel interference.

To solve such problems, adaptive antennas provided the following benefits over the conventional antennas systems [2].

- Increased coverage
- Improved link quality
- Increased capacity
- Reduced costs and increased return on investment
- Lower handset power consumption
- Assistance in user location by means of direction finding
- Can provide multipath dispersion, interference suppression, and Increased data rate
- Unlike conventional cellular antennas, which broadcast energy over the entire cell, adaptive antenna confines the broadcast energy to a narrow beam.
- Conventional antennas cause coupling of the hand and head but adaptive antennas do not cause coupling of the hand and the head
- Mitigation against dead zones around Base stations of adjacent channel FDD network operators
- Improved spectral efficiency
- It combines the signal it receives directly from the base station with the reflections of the same signal whereas a conventional handset normally tunes into the strongest signal it can find.
- It is possible to combine the signals from the antennas in a particular way that both the SNR (signal to noise ratio) and CIR (carrier to interference ratio) levels are improved.
- Limitations overcome in wireless communications systems by making use of multiple antennas in conjunction with computer algorithms. The signals are combined from multiple antennas to reduce interference. The desired signal is strengthened using algorithms that determine how to adjust the phase and amplitude of the signals from each antenna before the signals are combined.
- Research done on outdoor mobile communication systems indicates that addition of adaptive circuitry can overcome most of the impairments by the effects of multipath fading.
- Antenna Diversity at the handset in indoor environment results in improved radio link.

- In using more than one adaptive antenna, increase the number of users able to operate simultaneously in each frequency band.
- For the user, higher QOS, more reliable, secure communication, new services, and longer battery life.

Though adaptive antennas played a vital role to increase the performance of wireless communication, still as communication systems have progressively increased in complexity, many new methods have been investigated for increasing performance and capacity. It was incorporated to use adaptive antennas at handsets for improved performance and the effectiveness of a smart antenna system can be clearly examined by applying diversity and adaptive combining schemes at the handsets. Applying antenna diversity at the handsets can reduce capacity problems and co-channel interference.

Diversity techniques play a vital role in supporting high-speed connections over radio channels by mitigating the detrimental effects of multi-user interference and multipath fading. Multipath fading is a main obstacle for cellular radio to achieve reliable communication; an effective means to combat multipath fading is diversity combining, which relies on a simple principle. Namely, if a number of well-separated antennas are used to receive the same signal, it is unlikely that all received signals fade at the same time. Multiple antennas at the transmitter and receiver provide diversity in a fading environment. By employing multiple antennas, multiple spatial channels are created, and it is unlikely all the channels will fade simultaneously.

With the growth of demand for wireless communication, many researchers have taken the challenge to model wireless channels accurately. For proper and efficient implementation of future systems, emerging wireless systems must be able to exploit processing of spatial information. Multipath and time varying nature of the mobile radio channels pose a major design problem for mobile wireless systems. Smart antennas and systems used in position location are among the most popular new studies that require signal information such as the amplitude, phase, and angle-of-arrival (AOA) of multipath delay spreads. To test the performance of antenna arrays, an accurate description of the spatio-temporal channel model is required. Two statistical channel models known as Geometrically Based Single Bounce (GBSB) elliptical and GBSB circular are described in this thesis. In these models it is assumed that the multipath reflections are created by random placement of scatterers inside a region defined by a specific geometry. From the position of the scatterers, multipath delays, AOA and power levels are determined. Thus

these models provide a statistical description of the wideband spatio-temporal radio channel.

In practice, mobile communications environments have characteristics that cause the transmitted/received signal to fade (drop below a certain threshold) over time and distance. This characteristic is created because there are several time-delayed versions of the input signal transmitted (multipath) that travel their own paths and arrive in the same place as the original signal. Communication engineers attempt to use computer simulations to approximate channel characteristics so that a general idea can be obtained about the system performance (BER, SNR) at the input to the receiver [3].

1.2 Objectives of the thesis

The objectives of the thesis are:

- To calculate the BER of Matched Filter Receiver for AWGN channel.
- To calculate the BER of Matched Filter Receiver for 1-path Rayleigh Fading Channel and compare its performance with AWGN Channel.
- To calculate the BER of Matched Filter Receiver for 1-path Ricean, and Nakagami Fading Channel and compare their performance with 1-path Rayleigh Fading Channel
- To calculate the BER of Matched Filter Receiver for these statistical channel models with applied diversity combining techniques like EGC, MRC, and SC and compare their performance level.
- To achieve the BER of Matched Filter Receiver for 1-path spatial channel models like GBSB Elliptical and GBSB Circular Channels.
- To compare the performance level of the antenna systems for Matched Filter Receiver of the statistical channel models by varying the number of antenna elements with applied EGC, MRC, and SC.
- To compare the performance level of the spatial channel models with varying number of antenna elements with applied EGC, MRC, and SC.

The methodology to achieve these objectives is to run simulations to gather performance statistics of various micro diversity techniques. The system model is assumed to have a configurable number of fading branches, which are simulated by generating random processes. Signals received from these branches are input to the discrete matched filter and then combined using various diversity combining techniques. The resulting SNR is then converted to probability of bit error (or outage probability). The number of bits in

error is determined by comparing the output with the transmitted data stream. That is, the bit error rate is calculated as the ratio of number of bits in error to the total number of bits transmitted. The simulation only assumes that the branches receive independent fading paths and does not concern with its source (that is, it can be space, time or frequency diversity).

1.3 Organization of the report

In Chapter 2 a brief overview of the key words like smart antennas, diversity techniques, statistical and spatial channel models are mentioned along with a brief overview of key research papers is given to introduce the current state of research in this field. Chapter 3 describes various types of diversity and various diversity combining techniques. Also a comparison between various combining techniques have been made and proved through Matlab. Chapter 4 introduces single-state fading and gives a brief description of some popularly used single-state statistical fading channel models. The chapter also includes the assumptions and the iterative steps followed for the simulation process and the results obtained by the simulation applied on the diversity channel models. In chapter 5, the spatio-channel models, Geometrically based Single Bounce (GBSB) elliptical and GBSB circular, are described for micro and macro-cellular environments are described along with their advantages and disadvantages. The results obtained by the simulation applied on the diversity channel models are shown. Finally in chapter 6, the conclusion part of the thesis is outlined which is a result of the iterative work carried out on various diversity channel models.

Chapter-2

Multiple Antennas at Handsets

In this chapter, smart antennas at handsets are described in brief. Their specific needs at handsets are also mentioned. Diversity techniques at handsets are next discussed and nowadays as the emphasis is laid on the performance of handheld antenna arrays using diversity combining to mitigate the effect of fading due to multipath, the diversity combining techniques like EGC, MRC, and SC are also briefed down. The flat fading statistical and spatial channel models are also described in brief as these antenna diversities are most effective in these channels.

2.1 Introduction

Multiple access wireless communications is being deployed for next generation cellular networks. In achieving this objective, wireless system designers are faced with a number of challenges in addition to limited radio spectrum and a complex wireless environment (fading and multipath). Meeting the increasing demand for higher data rates, better Quality of Service (QoS), fewer dropped calls, higher network capacity and user coverage calls for novel techniques that improve spectral efficiency and link reliability. Many methods have been adopted to meet the desired demand; applying diversity at handsets is among the popular of them. This chapter mentions the keywords of the thesis in brief along with a brief overview of key research papers to introduce the current state of research in this field.

2.2 Smart antennas

Adaptive antenna technology at a cellular base station (BS) has been a subject of interest for the past many years. But, with ongoing advancements in the performance in the semiconductor technology, more powerful and smaller chipsets are now available to be used in the hand-held mobiles. In [4], literature search for some of the research and developments in the area of the smart antennas for handsets has been carried out. It was found that by using two diversity branches at handset a diversity gain of about 7 to 9 dB could be achieved. It was also found that an overall antenna gains in the order of 20 dB were achieved using interference rejection in an adaptive antenna array. Sufficient information is provided for the formulation of a statistical model of a smart antenna that represents the gain in the SINR that might be realizable using handsets with adaptive antennas instead of the conventional antennas.

Smart antenna technology is a promising means to overcome signal impairments in wireless personal communications. When spatial signal processing achieved through smart antennas is combined with temporal signal processing, the space-time processing can

mitigate interference and multipath to yield higher network capacity, coverage, and quality. A dual smart antenna system incorporated into handsets for the third generation wireless personal communication systems in which the two antennas separated by a quarter wavelength are discussed [5]. The effectiveness of a dual smart antenna system with diversity and adaptive combining schemes is examined in this dissertation.

The smart antenna is found to allow higher data rates on the network. Higher data rates between 20% to 100% could be used with the smart antennas. The improvement was found to be highest for low data rates and to decrease when high data rates are used.

2.3 Need of Adaptive Antennas at Handsets

Adaptive Antennas is a potential performance enhancement tool in a communications link that can be used at either end (transmitter or receiver) of the link in the form of beamforming or diversity operation. As wireless communication systems are evolving, service quality and capacity are becoming the prime importance. For reliable communication over a mobile radio channel, a system must overcome multipath fading, polarization mismatch, and interference. Antenna arrays can improve both reliability and capacity [6]. By using an antenna system, one with more than one antenna port in the handset, it is possible to combine the signals from the antennas in such a way that both the SNR level and the CIR level is improved.

Papers, investigations and research have been emerging concerning adaptive antennas on handsets dating from since 1997. In [2], adaptive antennas on the handsets have been discussed in terms of the benefits to the operator, regulator and user, the types of antennas and the advantages of having such antennas instead of the conventional antennas. New technologies under development i.e. small, solid-state antenna as manufactured by Antenova and the Quadrifilar helix antenna (QHA) produced by Surrey University and various other types have made the adaptive antenna on handsets a practical possibility. Benefits of using an adaptive antenna especially on the handset like increased coverage, data rates, reduced interference, increase in spectrum efficiency, which all are beneficial to the Radiocommunications Agency (RA), in terms of conserving the limited radio spectrum have been reported. For Operators like Orange, Vodafone and Hutchinson 3G, using these types of adaptive antennas could lead to a reduction in the number of base station masts needed for the 3G phone network as locating sites for these networks are difficult. The result of this is reduction in infrastructure cost, which will be beneficial and pleasing to the Operators.

2.4 Diversity Techniques at Handsets

Diversity techniques at the receiver, in which two or more copies of the same information-bearing signal are combined skillfully to increase the overall SNR, offer one of the greatest potential for radio link performance improvement to many of the current and future wireless technologies. For example, to meet stringent requirements for quality service requirements and spectrally efficient multilevel constellations, antenna (space) diversity is needed to offset penalty on the SNR due to fading and denser signal constellation. In addition, one of the most promising features of W-CDMA systems is their ability to resolve additional multipath (compared to “narrowband” CDMA systems), resulting in an increased multipath diversity, which can be exploited by rake reception. There are several ways in which we can provide the receiver with L -order diversity (i.e., fading replicas of the same information-bearing signal) [7].

Spatial diversity with receive antennas spaced typically ten or more wavelengths apart on cellular telephone towers is in widespread use. When mobile selects the base station, which is not shadowed when others are, the mobile can improve substantially the average SNR on the forward link. This is called macroscopic diversity, since the mobile is taking advantage of large separations between the serving base stations. In microscopic diversity, diversity antennas are separated by just a fraction of a meter. By selecting the best signal at all times, a receiver can mitigate small-scale fading effects [8].

It was incorporated to use adaptive antennas at handsets for improved performance and the effectiveness of a smart antenna system can be clearly examined by applying diversity and adaptive combining schemes at the handsets. Applying antenna diversity at the handsets can reduce capacity problems and co-channel interference. A mathematical framework for analyzing the average bit error rate performance of different selection diversity combining schemes over slow, frequency non-selective Rayleigh, Nakagami- m and Ricean fading channels is developed in [7]. The proposed analytical framework is sufficiently general to study the effects of dissimilar fading parameter and unequal mean received signal strengths across the independent diversity paths. The effect of branch correlation on the performance of a dual-diversity system is also studied. Extensive Monte-Carlo simulation runs have validated the accuracies of the analytical expressions.

Some researchers have proposed diversity combining at handheld radios and shown that significant performance gains can be achieved. In 1988, Vaughn concluded that with then-current technology, adaptive beamforming would work for units moving at pedestrian speeds but would be difficult for high-speed mobile units. In 1999, Braun, et al reported experiments in which data was recorded using a two-element handheld antenna array, and processed using diversity and optimum beamforming techniques. In [6] results of an

investigation into the performance of antenna arrays that can be mounted on handheld radios have been reported. The emphasis was laid on the investigation of the performance of handheld antenna arrays used with diversity combining (for mitigation of fading due to multipath), and with adaptive beamforming (for interference rejection). It was concluded that the signals received by the antennas in these handheld antenna arrays could be combined to provide 7-9 dB diversity gains against fading at the 99% reliability level in non line-of-sight multipath channels.

2.5 Diversity Combining Techniques

Diversity antennas provide two major benefits. First, reliability is improved in multipath channels. The fade level experienced on an average for a given outage probability (percentage down time) is decreased through diversity. Second, the overall average received signal power is increased. Systems that use diversity combining can provide 10dB or more diversity gain. The performance of diversity combiner is measured by diversity gain, which is difference in SNR between the output of a diversity combiner and the signal on a single branch measured at a given probability level. Diversity gain quantifies the improvement in SNR of a received signal that is obtained using signals from different receiver branches. It permits a direct comparison of improvement offered by multiple antenna sensors compared to a single one [8]. In this thesis three diversity techniques are studied viz. Selection Diversity, Maximal Ratio and Equal Gain Diversity.

Selection Diversity is the simplest diversity technique where gains of M pre-detection diversity branches are adjusted to provide the same SNR ratio for each branch. The receiver branch having the highest instantaneous SNR will be fed to detector circuit. In MRC, the signal in each branch is first co-phased and once the phase distortions are canceled out, the signal in each branch is weighted by a weighting factor proportional to the ratio of the carrier amplitude to the noise power for the i -th branch. In an EGC receiver, the received signal carriers are first co-phased as in the case of MRC and are then equally weighted by their amplitudes. In other words, the branch weights are all set to unity. The possibility of producing an acceptable signal from a number of unacceptable inputs is still retained [8].

The performance of MRC in both independent and correlated fading channels is analyzed in [9]. It examines MRC in independent and correlated Rayleigh fading channels. While channel correlation is a key factor in the performance of linear combining, significant performance improvement can still be achieved with semi-correlated fading channels with $\rho=0.6$, where ρ is the correlation.

2.6 Statistical Channel Models

Antenna diversity is most effective in flat fading channels. Equalizers or rake receivers employed in wideband radios cannot mitigate flat fading with a single antenna, but when combined with antenna diversity they can improve performance in both flat and frequency-selective fading channels. Pre-detection combining using space-diversity antenna array is commonly used to combat fading in mobile radio systems.

The statistical models are based on measurements made specifically for an intended communication system or spectrum allocation. A significant advantage of the wireless channel models is their flexibility, which means by changing the statistical parameters; the same model can be used to simulate the channel under different conditions. Propagating models have traditionally focused on predicting the average received signal strength at a given distance from the transmitter, as well as the variability of the signal strength in close spatial proximity to a particular location [8]. Multipath fading is due to the constructive and destructive combination of randomly delayed, reflected, scattered and diffracted signal components. This type of fading is relatively fast and is therefore responsible for the short-term signal variations. Depending on the nature of the radio propagation environment, there are different models describing the statistical behavior of the multipath-fading envelope [7].

The Rayleigh distribution is commonly used to describe the statistical time varying nature of the received envelope of a flat fading signal. The Rayleigh flat fading channel model assumes that the channel induces amplitude, which varies in time according to the Rayleigh distribution. This fading distribution could be applied to any scenario where there is no LOS path between transmitter and receiver antennas. When there are fixed scatterers or signal reflectors in the medium, in addition to randomly moving scatterers, the channel impulse response will have a nonzero mean value and its envelope will have a Rice distribution. This channel is said to be a Rician fading channel. The Nakagami-m distribution introduced by Nakagami was selected to fit empirical data and is known to provide a close match to some experimental data than the Rayleigh, Rician or lognormal distributions

An elaborate discussion of the small scale fading models, and antenna diversity combining techniques is outlined in [8]. A generalized mathematical framework has been developed in this report to compute the error probability of correlated dual diversity EGC systems.

In many cases the fading received at both the branches of a two-antenna element system is correlated because of the proximity of the antenna elements to each other. It is

also not uncommon for a diversity system to use antennas with different patterns or polarizations, this usually results in differences in average signal-to-noise ratios at both branches depending on which element is better matched to the signal environment. The performance of a diversity system depends greatly on the envelope correlation, average power imbalance and the combining scheme used on both branches. In [10], an analytical expression for the probability density function of the SNR at the output of a two-branch maximal ratio and selection diversity system is developed. The two branches are assumed to be Rayleigh fading, correlated, as well as of unequal signal-to-noise ratios. Measurements were made in Rayleigh fading channels and compared to the analytical results. The analytical cumulative distribution functions (derived using probability distributions) were found to be within 1 dB of the measured results (statistics obtained from time combining) for both maximal ratio and selection diversity attesting to the validity of the analytic results. The diversity gain for selection, maximal ratio, and equal gain combining for the 10% probability level is presented as a function of power imbalance and correlation between branches for a two-branch Rayleigh diversity system

2.7 Spatio-channel Models

Space-time geometrical channel models proved to be of significance in wireless communications as they provide spatial information (i.e. DOA, TOA) by which the performance of wireless communication systems and space-time systems (i.e., smart antennas, beamformers) can be analyzed. A comparative study of space-time geometrical channel models is presented in [11]. Based on the methods through which the models incorporate Doppler fading, we divide these models into two categories: models with oscillated scattering objects and models with unoscillated scattering objects. The main characteristics of each category have been studied using the existing models. This paper has provided a comparative and classifying study of the existing space-time geometrical channel models.

The main focus of the work in [12] has been to commercialize SIRCIM and SMRCIM and to implement the *Aisle Elliptical* and *Random Elliptical* AOA models. It outlines the development and implementation of these geometrically based single-bounce models for new angle-of-arrival (AOA) models in both indoor and outdoor wireless radio channel software simulation tools. Additionally, this thesis expounds upon the theory of propagation of electromagnetic waves in RF channels, the models utilized in channel simulation software, enhancements made within the software, and the future of the tools. Likewise, specifics of the user interface and the data supplied by the software are discussed.

In [13], a 2-D RAKE receiver for the uplink of the W-CDMA system is considered. The approach is to combine different PSA adaptive beamforming algorithms with a coherent MRC RAKE receiver. The reason for concentration on the PSA beamforming techniques is that the W-CDMA standard specifies pilot symbols in the uplink. These pilot symbols can be used for both beamformer weight calculation and channel estimation required for subsequent coherent RAKE combining. A detailed mathematical analysis of these PSA 2-D RAKE receivers with the uplink W-CDMA signal format is presented along with computer simulation test bed set up to compare the performance of these receivers in two different GBSB statistical channel environments with multipath Rayleigh fading. The BER performance versus both the number of users and E_b/N_0 of all these receivers are compared with varying number of spatial and temporal processing parameters.

Antenna array systems and RAKE receivers have the ability to recombine the information from multipath components of signals allowing detection with lower bit error rates while using lower transmit power. However, the design of these systems depends heavily on information about the typical channel response.

Chapter-3

Diversity Techniques

In this chapter, various diversity and diversity combining techniques are discussed in detail. The various types of diversity are used to provide the inputs to the diversity combiner. Now, since there are a variety of ways in which the independently fading signal branches can be combined, hence, the three most prevalent space diversity-combining techniques used are the Maximal Ratio Combining, Equal Gain Combining, and Selection Combining. These combining techniques are discussed and analyzed in detail in this chapter.

3.1 Introduction

Next generation wireless systems are being designed to provide ubiquitous broadband link access to information infrastructure. Diversity techniques play a vital role in supporting such high-speed connections over radio channels by mitigating the detrimental effects of multi-user interference and multipath fading. It was incorporated verify improved performance in both the statistical and spatial channel models. Diversity is known to reduce channel fading and increase the reliability of the transmitted signal. It is assumed that the signals received at the receiver are uncorrelated. Several diversity schemes were available to choose from including space, polarization, angle, frequency, and time. The independent channels in a fading channel environment are often referred to as diversity branches. Having multiple branches available at the receiver decreases the probability that the signals on each branch will all be in a deep fade [17].

3.2 Diversity Techniques

Diversity is a powerful communication receiver technique that provides wireless link improvement at relatively low cost. Unlike equalization, diversity requires no training overhead since the transmitter does not require a training sequence. Furthermore, there are wide ranges of diversity implementations, many of which are very practical and provide significant link improvement with little added cost. Diversity exploits the random nature of radio propagation by finding independent signal paths for communication. In virtually all applications, diversity decisions are made by the receiver, and are unknown to the transmitter.

The diversity concept can be explained simply. If one radio path undergoes a deep fade, another independent path may have a strong signal. By having more than one path to select from, both the instantaneous and average SNRs at the receiver may be improved.

3.3 Types of Diversity

In this section, we examine the type of diversity that can be used to provide the inputs to the diversity combiner. Most diversity systems are implemented in the receiver instead of the transmitter since no extra transmitter power is needed to implement the receiver diversity system. Since the path between the mobile and base is assumed to be reciprocal, diversity systems implemented in a mobile will work similarly to those in a base station. There are two general types of diversity schemes [21].

3.3.1 Macroscopic diversity scheme:

The Macroscopic diversity scheme is used for combining two or more long-term lognormal signals, which are obtained via independently fading paths received from two or more different antennas at different base-station sites. The local mean strength varies because of variations of terrain between the mobile transmitter and the base station receiver. If only one antenna site is used, the traveling mobile unit may not be able to transmit a signal to the base station at certain geographical locations because of terrain variations such as hills or mountains. Therefore, two separated antenna sites can be used to receive two signals and to combine them to reduce long-term fading. The selective combining technique is recommended in the macroscopic diversity scheme since other methods require coherent combining that is difficult to achieve when the receivers are some distance apart. Macroscopic diversity is often used in short-wave systems to reduce the effects of fading from the ionosphere. Cellular and PCS system achieve the same effect by handoffs to nearby cell sites when the signal strength becomes weak [22].

3.3.2 Microscopic diversity scheme:

The Microscopic diversity scheme is used for combining two or more short-term Rayleigh signals, which are obtained via independently fading paths received from two or more different antennas but only at one receiving co site. Once the diversity branches are created, any of the combining methods can be used. In mobile wireless communications, multipath fading can cause constructive and destructive interference. A popular method to mitigate the effects of multipath fading is diversity, a process of obtaining multiple independent signal branches through many dimensions including time, frequency, polarization, angle, and space [23].

3.3.2.1 Time Diversity:

Time diversity reception techniques are primarily applicable to the transmission of digital data over a fading channel. In time diversity, the same data are sent over the channel at time intervals of the order of the reciprocal of the baseband fade rate $f_b = 2f_m$. In mobile radio, the reciprocal fade rate can be expressed:

$$\tau \geq \frac{1}{2f_m} = \frac{1}{2\left(\frac{v}{\lambda}\right)} \quad (3.1)$$

The time separation increases as the fade rate decreases. Multiple diversity channels can be provided by successively transmitting the signal sample in each time slot. The sampling rate for voice transmission of a single channel is (2 x 4 kHz = 8kHz) [21]. For M-branch diversity, the sampling rate must be (M x 8 kHz), since the transmission delay spread is usually less than 20 μ s, which is much less than the inverse of the sampling rate:

$$f_s < \frac{1}{\Delta} \quad (3.2)$$

Hence, the sampling rate f_s is not limited by the time-delay spread. However, the minimum time separation between samples shown in Eq. (3.1) for diversity application may cause a serious problem, since f_m is a Doppler frequency, expressed:

$$f_m = \frac{V}{\lambda} \quad (3.3)$$

When the vehicle is stationary, $v=0$, and thus $f_m=0$. This means that the time separation μ_s is infinite. Therefore, the advantages of time diversity are lost when the vehicle is not moving. This is in sharp contrast to other diversity schemes, in which the branch separation is not a function of vehicle speed and thus the two diversity signals are independent over any value of v .

3.3.2.2 Frequency Diversity:

Frequency diversity is implemented by transmitting information on more than one carrier frequency. The rationale behind this technique is that frequencies separated by more

than the coherence bandwidth of the channel will be uncorrelated and will thus not experience the same fades. Theoretically, if the channels are uncorrelated, the probability of simultaneous fading will be product of the individual fading probabilities [17].

Frequency diversity is often employed in microwave line-of-sight links, which carry several channels in a frequency division multiplex mode (FDM). Due to tropospheric propagation and resulting refraction, deep fading sometimes occurs. In practice, 1:N protection switching is provided by a radio licensee, wherein one frequency is nominally idle but is available on a stand-by basis to provide frequency diversity switching for any one of the N other carriers (frequencies) being used on the same link, each carrying independent traffic. When diversity is needed, the appropriate traffic is simply switched to the backup frequency. This technique has the disadvantage that it not only requires spare bandwidth but also requires that there be as many receivers as there are channels used for the frequency diversity.

3.3.2.3 Polarization Diversity:

Signals transmitted in either horizontal or vertical electric fields are uncorrelated at both the mobile and Basestation receivers. The horizontal and vertical polarization components, E_x and E_y , transmitted by two polarized antennas at the base station and received by two polarized antennas at the mobile unit, can provide two uncorrelated fading signals. Polarization diversity results in a 3-dB power reduction at the transmitting site since the power must be split into two different polarized antennas. The decorrelation for the signals in each polarization is caused by multiple reflections in the channel between the mobile and base station. After sufficient random reflections, the polarization state of the signal will be independent of the transmitted polarization. In practice, however, there is some dependence of the received of the received polarization on the transmitted polarization [22].

3.3.2.4 Angle Diversity:

When the operating frequency is greater than 10 GHz, the scattering of the signals from transmitter to receiver generates received signals from different directions that are uncorrelated with each other. Thus, two or more directional antennas can be pointed in different directions at the receiving site and provide signals for a combiner. This scheme is more effective at the mobile unit than at the base station since the scattering is from local buildings and vegetation and is more pronounced at street level than at the height of base station antennas.

3.3.2.5 Space Diversity:

Space Diversity, also known as antenna diversity, is one of the most popular forms of diversity used in wireless systems. Conventional wireless systems consist of an elevated base station antenna and a mobile antenna close to the ground. The existence of a direct path between the transmitter and the receiver is not guaranteed and the possibility of a number of scatterers in the vicinity of the mobile suggests a Rayleigh fading signal. Two antennas separated physically by a short distance d can provide two signals with low correlation between their fades. The separation d in general varies with antenna height h and with frequency. The higher the frequency, the closer the two antennas can be to each other. Typically a separation of a few wavelengths is enough to obtain uncorrelated signals.

3.4 Basic Diversity Combining Methods:

The collection of independently fading signal branches can then be combined in a variety of ways to improve the received SNR. Since the chance of having two deep fades from two uncorrelated signals at any instant is rare, combining them can reduce the effect of the fades. The three most prevalent space diversity-combining techniques are SC, EGC, and MRC. MRC co-phases the signal branches, weights them according to their respective SNRs, and then takes their sum. MRC is the most complex combining technique, but also yields the highest SNR. The analysis of all of these diversity techniques is presented here.

3.4.1 Selection diversity:

Selection diversity is the simplest of all the diversity schemes. It is based on the probability that the received signals are greater than a threshold. As shown in fig 3.1 an ideal selection combiner chooses the signal with the highest instantaneous SNR of all the branches, so the output SNR is equal to that of the best incoming signal and makes it available to the receiver at all times. Multiple branches will improve the probability of having a larger SNR at the receiver [3]. A block diagram of SC is given in figure 3.1

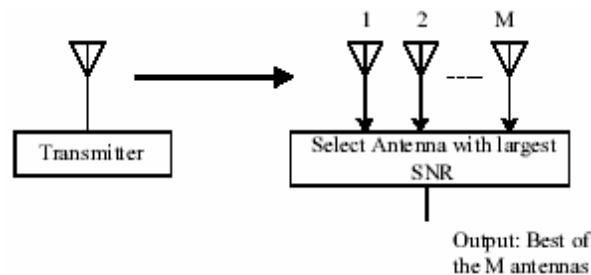


Fig. 3.1 Selection Diversity

We assume that the signal received by each diversity branch is statistically independent of the signals in other branches and is Rayleigh distributed with equal mean

signal power P_0 . The probability density function of the signal envelope, on branch i , is given by [22]

$$p(r_i) = \frac{r_i}{P_0} e^{-r_i^2/2P_0} \quad (3.4)$$

where $2P_0 = \text{mean-square signal power per branch} = \langle r_i^2 \rangle$ and

$r_i^2 = \text{Instantaneous power in the } i\text{-th branch.}$

Let $\xi_i = r_i^2/2P_0$ and $\xi_0 = (2P_0)/(2N_i)$, where N_i is the noise power in the i -th branch.

$$\therefore \frac{\xi_i}{\xi_0} = r_i^2/2P_0 \quad (3.5)$$

The probability density function for ξ_i is given by

$$p(\xi_i) = \frac{1}{\xi_0} e^{-\xi_i/\xi_0} \quad (3.6)$$

We assume that the signal in each branch has a constant mean; thus, the probability that the SNR on any one branch is less than or equal to any given value ξ_g is given by

$$P[\xi_i \leq \xi_g] = \int_0^{\xi_g} p(\xi_i) d\xi_i = 1 - e^{-\xi_g/\xi_0} \quad (3.7)$$

Therefore, the probability that the SNRs in all branches are simultaneously less than or equal to ξ_g is given by

$$P_M(\xi_g) = P[\xi_1, \xi_2, \dots, \xi_M \leq \xi_g] = \left[1 - e^{-\xi_g/\xi_0} \right]^M \quad (3.8)$$

The plots of the results for $M=1, 2$, and 4 are shown in figure 3.2

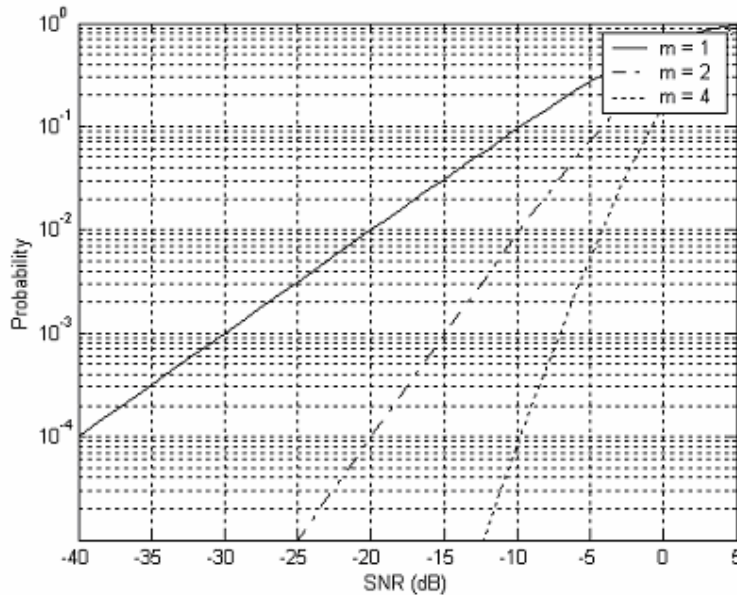


Fig. 3.2 Probability for different Values of M-Selection Combiner

3.4.2 Maximal ratio Combining:

MRC presents the receiver with a signal-to- noise ratio that is the direct sum of all individual SNRs in the branches as shown in figure 3.3. The main drawback of using MRC is that the signal level and noise power at each branch needs to be correctly estimated for all instances in time [3].

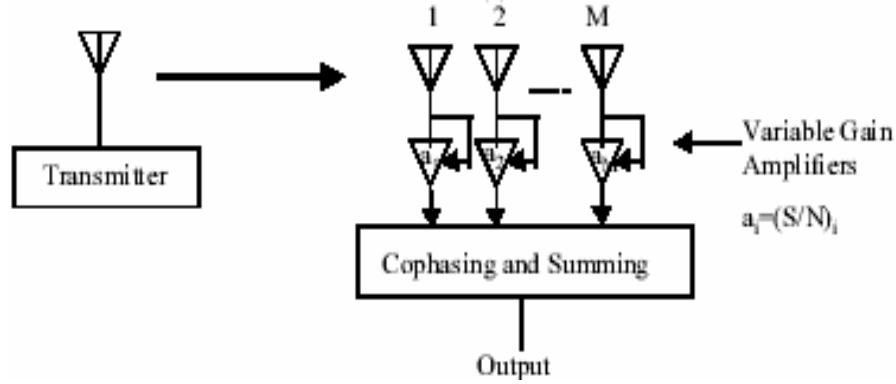


Fig. 3.3 Maximal Ratio Combining

The M signals are weighted proportional to their signal voltage-to-noise power ratios and then summed [22].

$$r_M = \sum_{i=1}^M a_i r_i(t) \quad (3.9)$$

Since noise in each branch is weighted according to noise power,

$$\overline{n_i^2(t)} = \sum_{j=1}^M \sum_{i=1}^M a_i a_j \overline{n_i(t) n_j(t)} \quad (6.10)$$

The average noise power,

$$N_T = \sum_{i=1}^M a_i^2 \overline{n_i^2(t)} = 2 \sum_{i=1}^M |a_i|^2 N_i \quad (6.11)$$

where $\overline{n_i^2(t)} = 2N_i$

The probability that $\xi_M \leq \xi_g$ is given by:

$$P(\xi_M \leq \xi_g) = 1 - e^{-\frac{\xi_g}{\xi_0}} \sum_{K=1}^M \frac{\left(\frac{-\xi_g}{\xi_0}\right)^{K-1}}{(K-1)!} \quad (6.12)$$

$$P(\xi_M > \xi_g) = e^{-\frac{\xi_g}{\xi_0}} \sum_{K=1}^M \frac{\left(\frac{\xi_g}{\xi_0}\right)^{K-1}}{(K-1)!} \quad (6.13)$$

The plot of P for M=1,2, and 4 is shown in figure 3.4

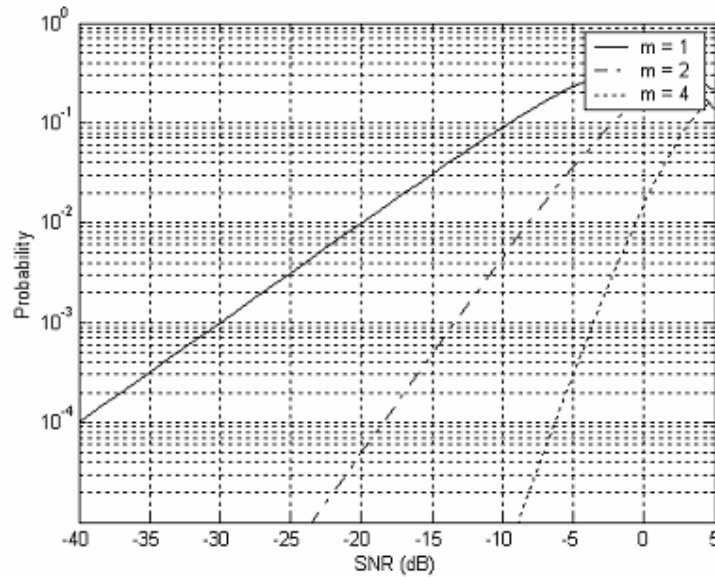


Fig. 3.4 Probability for different Values of Maximal Ratio Combiner

3.4.3 Equal Gain Combining:

EGC diversity receiver is of practical interest because of its reduced complexity relative to optimum maximal ratio combining scheme while achieving near-optimal performance [3]. It is the sum of all the signals received in order to increase the available SNR at the receiver. The gain of all of the branches is set to a particular value that does not change which is in contrast to MRC. The block diagram of EGC is shown in figure 3.5

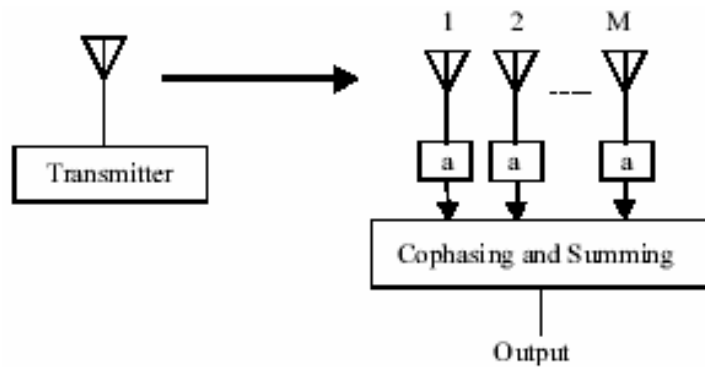


Fig. 3.5 Equal Gain Combining

EGC is similar to MRC, but there is no attempt to weight the signal before addition; thus $a_i = 1$. The envelope of the output signal with all $a_i = 1$ is given by [22]

$$r = \sum_{i=1}^M r_i \quad (3.14)$$

and the mean output is given as:

$$\overline{\xi_M} = \frac{1}{2} \frac{\left[\sum_{i=1}^M r_i \right]^2}{\sum_{i=1}^M N_i} \quad (6.15)$$

For $M=2$, the probability P can be written in closed form as :

$$P(\xi_M \leq \xi_g) = 1 - e^{-\left(\frac{2\xi_g}{\xi_0}\right)} - \sqrt{\pi \left(\frac{\xi_g}{\xi_0}\right)} e^{-\frac{\xi_g}{\xi_0}} .erf \sqrt{\frac{\xi_g}{\xi_0}} \quad (6.16)$$

For $M > 2$, the probability can be obtained by numerical integration techniques. The plot of probability $P(\xi_M \leq \xi_g)$ is given in figure 3.6

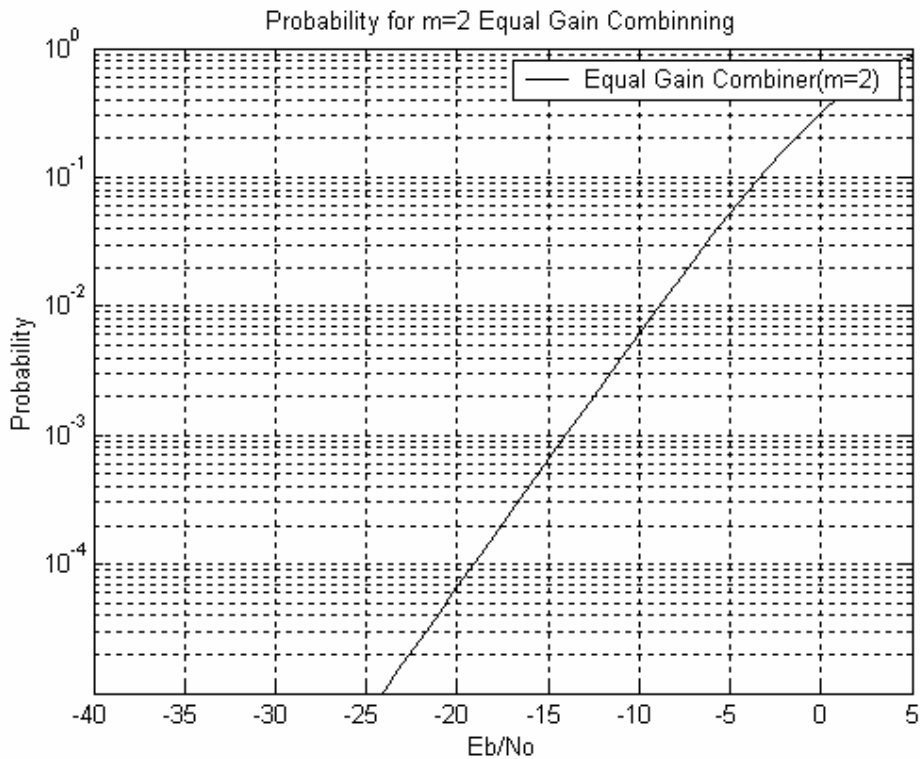


Fig. 3.6 Probability for M=2 Equal-Gain Combiner

The data for the SC, MRC, and EGC is compared in figure 3.7. It can be seen that selection diversity scheme has the poorest performance and maximal ratio the best. The performance of EGC is only marginally inferior to MRC. The implementation complexity for EGC is significantly less than the MRC because of the requirement of correct weighing factors.

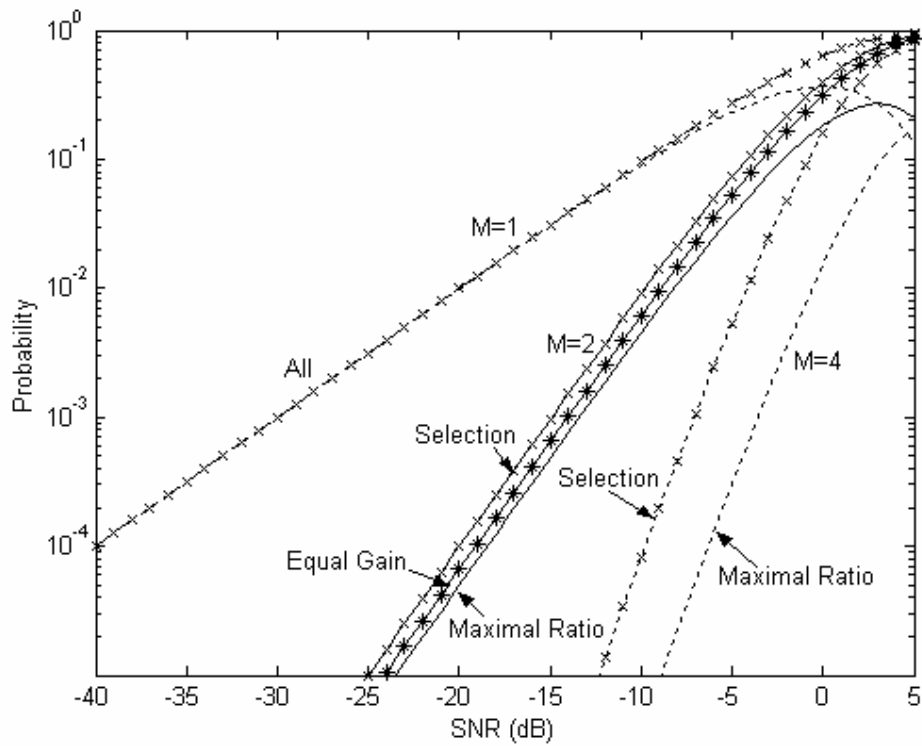


Fig. 3.7 Performance Comparison Improvement of Various Combining Techniques

Hence, the basic idea of diversity reception is that, if two or more independent samples of a signal are taken, then these samples will fade in an uncorrelated manner. This means that the probability of all the samples being simultaneously below a given level is much less than the probability of any individual sample being below that level. The probability of M samples all being simultaneously below a certain level is p^M , where p is the probability that a single sample is below the level. Thus, it can be seen that a signal composed of a suitable combination of various samples will have much less severe fading properties than any individual sample alone.

In this chapter, firstly the small scale fading is discussed. Small scale fading refers to the rapid fluctuations of the amplitudes, phases, or multipath delays of a radio signal over a short period of time or travel distance. Since the propagation models focus on predicting the average received signal strength and hence characterize the rapid fluctuations at a given distance from the transmitter, the small scale statistical fading channel models are then considered. The analysis of these models with applied diversity techniques are also analyzed in this chapter.

4.1 Introduction

Radio-wave propagation through wireless channels is a complicated phenomenon characterized by various effects, such as multipath and shadowing. A precise mathematical description of this phenomenon is either unknown or too complex for tractable communication systems analyses. However, considerable efforts have been devoted to the statistical modeling and characterization of these different effects. The result is a range of relatively simple and accurate statistical models for fading channels, which depend on the particular propagation environment and the underlying communication scenario.

The statistical models are based on measurements made specifically for an intended communication system or spectrum allocation. A significant advantage of the wireless channel models is their flexibility, which means by changing the statistical parameters; the same model can be used to simulate the channel under different conditions. Propagation models have traditionally focused on predicting the average received signal strength at a given distance from the transmitter, as well as the variability of the signal strength in close spatial proximity to a particular location. Large-scale propagation models are the models that predict the mean signal strength for an arbitrary transmitter-receiver (T-R) separation, thereby estimating the radio coverage of a transmitter [9]. On the other hand, propagation models that characterize the rapid fluctuations of the received signal strength over very short travel distances (a few wavelengths) or short time durations (on the order of seconds) are called small-scale or fading models.

4.2 Small scale fading

Small scale fading refers to the rapid fluctuations of the amplitudes, phases, or multipath delays of a radio signal over a short period of time or travel distance, so that large-scale path loss effects may be ignored. Fading is caused by interference between two or more versions of the transmitted signal, which arrive at the receiver at slightly different times. These waves, called multipath waves, combine at the receiver antenna to give a resultant signal, which can vary widely in amplitude and phase, depending on the distribution of the intensity and relative propagation time of the waves and the bandwidth of the transmitted signal. In small-scale fading, the received signal power may vary by as much as three or four orders of magnitude (30 or 40 dB) when the receiver is moved by only a fraction of a wavelength

In built-up urban areas, fading occurs because the heights of the mobile antennas are well below the height of surrounding structures, so there is no single LOS path to the base station. Even when a LOS exists, multipath still occurs due to reflections from the ground and surrounding structures. The signal received by the mobile at any point in space may consist of a large number of plane waves having randomly distributed amplitudes, phases, and angles of arrival. These multipath components combine vectorially at the receiver antenna, and can cause the signal received by the mobile to distort or fade. Even when a mobile receiver is stationary, the received signal may fade due to movement of surrounding objects in the radio channel [17].

If the motion is considered to be only due to that of the mobile, with objects to be static, then the fading is purely a spatial phenomenon. The spatial variations of the resulting signal are seen as temporal variations by the receiver as it moves through the multipath field. Due to the constructive and destructive effects of multipath waves summing at various points in space, a receiver moving at high speed can pass through several fades in a small period of time.

Another ill effect of non-stationary mobile channel is the Doppler shift, which describes the apparent frequency shift that each multipath experiences due to relative motion between the mobile and the base station. Multipath, ISI and Doppler shift are all related to variability that is introduced by the mobility of the user and the wide range of environments that signals pass through. The cumulative effect of these phenomena is the severe degradation in received signal strength, poor mobile receiver performance and hence, unsatisfactory QoS of the wireless system. Figure 4.1 shows the multipath propagation of the signal

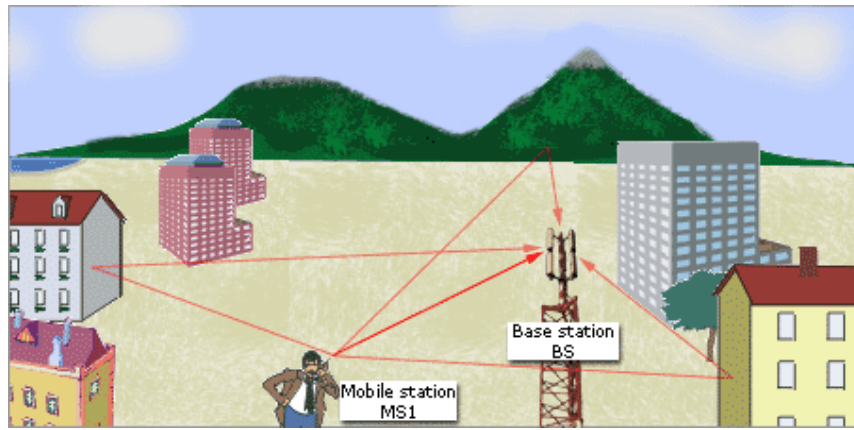


Fig. 4.1 Multipath propagation of a signal

4.3 Types of small scale fading

When the waves of multipath signals are out of phase, reduction in signal strength or fade can occur. The type of fading experienced by a signal propagating through a mobile radio channel depends on the nature of the transmitted signal with respect to the characteristics of the channel. Depending on the relation between the signal parameters (such as bandwidth, symbol period, etc.) and the channel parameters (such as rms delay spread and Doppler spread), different transmitted signals will undergo different types of fading. Fade zones tend to be small, multiple areas of space within a multipath environment that cause periodic attenuation of a received signal for users passing through them. In other words, the received signal strength will fluctuate downward, causing a momentary, but periodic, degradation in quality.

The small-scale signal fading due to the time dispersion and frequency dispersion mechanisms in a mobile channel could be classified into four major categories depending on the nature of the transmitted signal, the channel and the mobile velocity.

4.3.1 Fast Fading

In a fast fading channel, the channel impulse response changes rapidly within the symbol duration. That is, the coherence time of the channel is smaller than the symbol period of the transmitted signal. This causes frequency dispersion due to Doppler spreading, which leads to signal distortion. Fast fading channel only deals with the rate of change of the channel due to motion. In practice, fast fading only occurs for very low data rates.

4.3.2 Slow Fading

In a slow fading channel, the channel impulse response changes at a much slower rate than the transmitted baseband signal. The channel may be assumed to be static over one or several reciprocal bandwidth intervals. In the frequency domain, this implies that the Doppler spread of the channel is much less than the bandwidth of the baseband signal.

4.3.3 Frequency Selective Fading

The channel creates frequency selective fading on the received signal if the channel possesses a constant-gain and linear phase response over a bandwidth that is smaller than the bandwidth of transmitted signal. Under such conditions, the channel response has a multipath delay spread which is greater than the reciprocal bandwidth of the transmitted message waveform. When this occurs, the received signal includes multiple versions of the transmitted waveform, which are attenuated and delayed in time, and hence the received signal is distorted. When viewed in frequency domain, certain frequency components in the received signal spectrum have greater gains than others. The spectrum of the transmitted signal, for frequency selective fading, has a bandwidth greater than the coherence bandwidth of the channel.

Frequency selective fading channel models are very difficult to model since each multipath must be modeled and the channel must be considered to be a linear filter. Therefore, these models are typically developed from the wideband multipath measurements. However, when analyzing mobile communication systems, statistical impulse response models such as the two-ray Rayleigh fading model are generally used. In two-ray Rayleigh fading model, the consideration is that the impulse response of the channel is made up of two delta functions that fade independently and have sufficient time delay between them to induce frequency selective fading upon the applied signal [17].

4.3.4 Flat Fading

The received signal will undergo flat fading channel if the mobile radio channel has a constant gain and linear phase response over a bandwidth, which is greater than the bandwidth of the transmitted signal. The multipath structure of the channel is such that the spectral characteristics of the transmitted signal are preserved at the receiver but the strength of the received signal changes with time due to fluctuations in the gain of the channel caused by multipath.

Flat fading channels are also known as narrowband channels since the bandwidth of the applied signal is narrow as compared to the channel flat fading bandwidth. Typical flat fading channels cause deep fades and thus require a higher transmitter power of 20 or 30 dB to achieve low bit error rates during times of deep fades.

4.4 Fading channel models

Multipath fading is due to the constructive and destructive combination of randomly delayed, reflected, scattered and diffracted signal components. This type of fading is relatively fast and is therefore responsible for the short-term signal variations. Depending on

the nature of the radio propagation environment, there are different models describing the statistical behavior of the multipath-fading envelope. The Rayleigh, Ricean and Nakagami are the most commonly used statistical models to represent small-scale fading phenomenon

4.4.1 Rayleigh Fading Channel:

The Rayleigh distribution is commonly used to describe the statistical time varying nature of the received envelope of a flat fading signal, or the envelope of an individual multipath component. In the Rayleigh flat fading channel model, it is assumed that the channel induces amplitude, which varies in time according to the Rayleigh distribution. Figure 4.2 shows the representation of the Rayleigh fade effect on a signal [9].

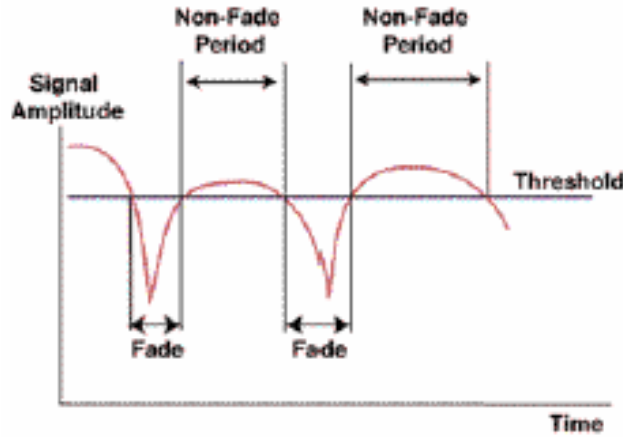


Fig. 4.2 Illustration of Rayleigh fade effect on a signal

When the channel impulse response is modeled as a zero-mean complex-valued Gaussian process, the envelope at any instant is Rayleigh-distributed. The Rayleigh distribution of a received complex envelope of a signal $z(t) = |r(t)|$ at any time t is given as

$$p_z(x) = \frac{x}{\sigma^2} e^{\left(\frac{-x^2}{2\sigma^2}\right)} \quad (x \geq 0) \quad (4.1)$$

where σ is the root mean square value of the received voltage signal before envelope detection, and σ^2 is the time-average power of the received signal before envelope detection. It is well known that the envelope of the sum of two quadrature Gaussian noise signals obeys a Rayleigh distribution. This fading distribution could be applied to any scenario where there is no LOS path between transmitter and receiver antennas.

4.4.2 Ricean Fading Channel

When there is a dominant stationary (non-fading) signal component present, such as LOS propagation path, the small-scale fading envelope distribution is Ricean. In such a situation, random multipath components arriving at different angles are superimposed on a

stationary dominant signal. At the output of an envelope detector, this has the effect of adding a dc component to the random multipath. The effect of a dominant signal arriving with many weaker multipath signals gives rise to the Ricean distribution. As the dominant signal becomes weaker, the composite signal resembles a noise signal, which has an envelope that is Rayleigh. Thus, the Ricean distribution degenerates to a Rayleigh distribution when the dominant component fades away.

With fixed scatterers or signal reflectors in the medium, in addition to randomly moving scatterers, the channel impulse response will have a non-zero mean value and its envelope will have a Rice distribution. This channel is said to be a Ricean Fading Channel. For a multipath fading channel containing a specular or LOS component, the complex envelope of the received signal can be given by the Ricean distribution

$$p(r) = \begin{cases} \frac{r}{\sigma^2} e^{-\frac{(r^2+A^2)}{2\sigma^2}} I_0\left(\frac{Ar}{\sigma^2}\right) & \text{for } (A \geq 0, r \geq 0) \\ 0 & \text{for } (r < 0) \end{cases} \quad (4.2)$$

where A denotes the peak amplitude of the dominant or LOS signal and $I_0(\cdot)$ is the zeroth order modified Bessel function of the first kind. The Rician distribution is often described in terms of a parameter K called Rician factor, which is defined as the ratio between the deterministic signal power and the variance of the multipath.

Generation of Rayleigh and Ricean Fading Parameters

The method of filtered noise is used to generate channel coefficients with the specified distribution and spectral power density. For each tap a set of complex zero-mean Gaussian distributed numbers is generated with a variance of 0.5 for the real and imaginary part, so that the total average power of this distribution is 1. This yields a normalized Rayleigh distribution (equivalent to Rice with $K=0$) for the magnitude of the complex coefficients. If a Ricean distribution ($K>0$ implied) is needed, a constant path component $|m|$ has to be added to the Rayleigh set of coefficients. The ratio of powers between this constant part and the Rayleigh (variable) part is specified by the K -factor. For this general case, we show how to distribute the power correctly by first stating the total power P of each tap [18]:

$$P = |m|^2 + \sigma^2 \quad (4.3)$$

where m is the complex constant and σ^2 the variance of the complex Gaussian set. Second, the ratio of powers is

$$K = \frac{|m|^2}{\sigma^2} \quad (4.4)$$

From these equations, we can find the power of the complex Gaussian and the power of the constant part as

$$\sigma^2 = P \frac{1}{K+1}; \quad \text{and} \quad |m|^2 = P \frac{K}{K+1} \quad (4.5)$$

Now, with the help of the specified powers, Ricean channel coefficients can be calculated.

K-Factor — The fading signal magnitude follows a Rice distribution, which can be characterized by two parameters: the power P_c of constant channel components and the power P_s from scatter channel components. The ratio of these two (P_c/P_s) is called the Ricean K -factor. The worst-case fading occurs when $P_c = 0$ and the distribution is regarded as Rayleigh distribution ($K = 0$). The K -factor is an important parameter in system design since it relates to the probability of a fade of certain depth. Both fixed and mobile communications systems have to be designed for the most severe fading conditions for reliable operation (i.e., Rayleigh fading).

4.4.3 Nakagami Fading Channel

The Nakagami distribution is selected to fit empirical data and is known to provide a close match to some experimental data than the Rayleigh, Ricean or lognormal distributions. The Nakagami distribution is often used to model multipath fading as it can model fading conditions that are either more or less severe than Rayleigh fading. When $m=1$, Nakagami distribution becomes the Rayleigh distribution, when $m=1/2$ it becomes a one-sided Gaussian distribution and when $m \rightarrow \infty$ the distribution becomes an impulse (no fading). Even Rice distribution can be closely approximated using Nakagami parameter m via the relationship $m = (K+1)^2/(2K+1)$ [8].

Considering a receiver with M diversity branches, let the received instantaneous signal A_k at the k^{th} branch be characterized by the Nakagami distribution. The Nakagami distribution describes the received envelope $z(t) = r(t)$ by a central chi-square distribution with m degrees of freedom, i.e. [19],

$$p(A_k) = \frac{2}{\Gamma(m_k)} \cdot \left(\frac{m_k}{\Omega_k} \right)^{m_k} \cdot A_k^{2m_k-1} \cdot e^{-\frac{m_k}{\Omega_k} A_k^2}, \quad k = 1, 2, \dots, M \quad (4.6)$$

where $\Gamma(\cdot)$ is the Gamma function, $\Omega_k = \overline{A_k^2}$ is the average power on k^{th} branch, m_k is the fading parameter.

Generation of Nakagami Channel Fading parameters

A Rayleigh distributed 'r' is considered where

$$\begin{aligned} |r| &= \text{Mag}(r) \\ \angle r &= \text{phase}(r) \end{aligned} \quad (4.7)$$

For the general case, the channel coefficients with Nakagami distribution can be calculated as

$$a = \sqrt{\log\left(\frac{1}{1-|r|}\right)^{1/m}} \quad (4.8)$$

where

m is the Nakagami-m fading parameter, and $0.65 \leq m \leq 10$, inf (positive real).

4.5 Diversity Techniques in Statistical Fading Channel Models

Antenna diversity is most effective in flat fading channels and pre-detection combining using space-diversity antennas array is commonly used to combat fading in mobile radio systems. The concepts of basic diversity combining techniques have already been discussed in chapter-3. Hence in this section of chapter-4, diversity combining techniques as applied to the fading channel models are analyzed. Also the simulation results to evaluate the performance of smart antenna system at handsets with applied diversity combining techniques are presented.

4.6.1 Simulation of Diversity Techniques

Assumptions

Before running our simulations, some assumptions in models are be made for simplification and requirements. These are:

1. The first assumption is that our fading channels do not introduce phase distortion, and introduce only magnitude attenuation. Therefore, in our simulation of a fading channel processes, we've only considered the magnitude of the in-phase and quadrature random variables.
2. Another assumption considers the characteristics of the channel. We have assumed a flat fading channel model. This means we assumed that the multipath structure of the channel is such that the spectral characteristics of the transmitted signal are preserved. However, the strength of the received signal varies with time, due to fluctuations in the gain of the channel caused by the multipath signals.
3. The final assumption that we made considered the fact that we have perfect knowledge of the channel. Since we know what the channel is, this means that there is no need to do channel estimation at the receiver.

Iterative steps followed for the simulation process

The following sequence of steps were applied to the coefficients obtained from various channel models:

- A binary data sequence that has equally probable bits of '1' and '0' is generated and the data sequence so obtained is encoded into NRZ format using the following equation:

$$x = 2 \cdot x - 1$$

- The so obtained NRZ data is then sampled at 16 times the data rate.
- It is also very important to understand that a 10,000 bit random source was used in all simulations.
- The NRZ data stream is transmitted over an Additive White Gaussian Noise (AWGN) Channel by adding white Gaussian noise of variance σ_N^2 .
- The received signal is compared with the signal used for encoding the bits 1 and 0 using the matched filter. The discrete matched filter can be expressed by the equation

$$Z = \frac{1}{N} \sum_{n=(k-1)N+1}^{kN} (Y_n)(A - (-A))$$

where

Z is the decision variable,

Y_n is the received NRZ data corrupted by noise, and

N is the number of samples/bit (N=16 in this case)

- Using the matched filter, the error probability error for AWGN is calculated as

$$P_e = Q \left(\frac{A}{\sqrt{\frac{\sigma_N^2}{16}}} \right)$$

since A=1,

$$\sigma_N^2 = \frac{8}{E_b/N_0}$$

where

the output of the channel is represented as

$$Y(t) = \sum A_k r_k p(t - tT_b) + n(t)$$

where

A_k is the transmitted bit sequence,

r_k is a sequence of independent random variables

- For 1-path Rayleigh Fading Channel, the BER is calculated as

$$P_e = \left(\frac{1}{2}\right) \frac{1}{\left(1 + \frac{E_b}{N_0}\right)}$$

- For two or more paths, diversity-combining schemes are used. NRZ data is multiplied by a factor $\frac{1}{\sqrt{M}}$ to calculate the average power in each branch where M is the number of branches.
- The three diversity combining schemes used are

1. Selective Maximum Combining

The random variables $Z_{1k}, Z_{2k}, \dots, Z_{nk}$ obtained from the output of the n discrete matched filters are compared and the maximum from them is passed to the decision block.

$$\begin{aligned} Z_k &= Z_{1k} && \text{if } |Z_{1k}| > |Z_{2k}| > \dots |Z_{nk}| \\ Z_k &= Z_{2k} && \text{if } |Z_{2k}| > |Z_{1k}| > \dots |Z_{nk}| \\ &\vdots && \\ Z_k &= Z_{nk} && \text{if } |Z_{nk}| > |Z_{1k}| > \dots |Z_{(n-1)k}| \end{aligned}$$

2. Equal Weight Combining

Associating equal weights to the random variables combines them as follows

$$Z_k = Z_{1k} + Z_{2k} + \dots + Z_{nk}$$

This is passed to the decision block. Z_k is '1' if $Z_k \geq 1$ or '0' if $Z_k < 0$

3. Maximal Ratio Combining

The random variables according to the expression

$$Z_k = r_{1k}Z_{1k} + r_{2k}Z_{2k} + \dots + r_{nk}Z_{nk}$$

- The output from the decision device is obtained by applying the above diversity combining schemes. By comparing this output with the transmitted binary data stream, number of bits in error is determined. The BER is calculated as the ratio of No. of bits in error to the total no. of bits transmitted and is plotted versus $\frac{E_b}{N_0}$ in dB.

4.6 Results and Discussion

- In table 4.1 the simulation results of Rayleigh Fading Channel with three diversity Combining Schemes are summarized for SNR of 1dB, 5dB and 10dB. It can be seen that BER for 1-path channel is higher than for 2-path channel with applied diversity schemes. , Hence, it can be inferred that the performance of antennas systems improves by applying diversity at the receivers.
- Also the performance level of the three diversity-combining schemes applied at the receiver can be compared from table 4.1 for Rayleigh Fading Channel. The calculated values of BER at different values of SNR show that Maximal Ratio Combining has the best performance as compared to other diversity combining techniques
- The values of BER for Ricean Fading Channel for the SNR of 1dB, 5dB, and 10dB are tabulated in table 4.2. As can be concluded from the table that the probability of error decreases as the antenna system is updated from 1-path to 2-path. Also, by applying the diversity combining techniques at the receiver the performance of the antennas system increases. It can be inferred from table 4.2 that, amongst the three diversity combining techniques applied, MRC gives the best performance and Selective Maximum the worst. The performance of EGC however lies between the two.
- The comparison between the Nakagami fading for 1-path and 2-path channels is summarized in table 4.3. Again it can be concluded that the performance of 2-channel antenna system is better than the 1-path channel models. Also by applying the diversity combining techniques, the performance improves and that the MRC gives the best performance as compared to the other two schemes.
- The variation in the bit error rate for Rayleigh Fading channel with the increase in no. of elements is shown in table 4.4. It can be seen from the table 4.4 that as the no. of antenna elements increases from 2 to 4 along with the SNR, the bit error rate decreases i.e. the channel gives better performance. It can also be concluded that MRC gives the best performance for each case of the no. of antenna elements.
- The BER values at different SNRs for Ricean Fading Channel with different number of antenna elements are summarized in table 4.5. It can be easily concluded from the table that the probability of error improves as number of elements increases at the receiver along with the SNR.
- Table 4.6 compares the bit error rate for Ricean Fading Channel. Even in this case the BER improves with the increment in the no. of the antenna elements

- Figure 4.3 shows the variation of BER against SNR for AWGN channel and the 1-path Rayleigh fading Channel. It can be seen that the BER for AWGN is less than 1-path Rayleigh Fading Channel due to fading. Also, in Rayleigh fading channel the additive white Gaussian Noise is present so the performance degrades further.
- Figure 4.4 shows the BER variations for 1-path Rayleigh fading channel and Figure 4.5 shows the BER variations for Rayleigh Fading Channel using second order diversity Combining Schemes. It can be seen that probability of error for 1-path channel is higher than for the channel with applied diversity schemes. Hence, it can be inferred from fig. 4.4 and fig. 4.5 that the performance of antennas systems improves by applying diversity at the receivers. It can also be concluded from figure 4.5 that among the three diversity techniques applied MRC shows the best performance and SC the worst.
- Fig. 4.6 and 4.7 shows the variation of BER with SNR for Ricean Fading 1-path and 2-path diversity Combining Schemes, respectively. As can be concluded from the graph that the probability of error decreases as the antenna system is updated from 1-path to 2-path. Also, by applying the diversity combining techniques at the receiver the performance of the antennas system increases. It can be inferred that, amongst the three diversity combining techniques applied, MRC gives the best performance and SC the worst. The performance of EGC however lies between the two.
- The comparison between the Nakagami fading for 1-path and 2-path channels is shown in figures 4.8 and 4.9 respectively. Again it can be concluded that the performance of 2-channel antenna system is better than the 1-path channel models. Also by applying the diversity combining techniques, the performance improves and that the MRC gives the best performance as compared to the other two schemes. However it can be seen that EGC and SC have almost the same level of performance but highly inferior to MRC.
- Figure 4.10 shows the variations of BER with SNR for the Equal Gain Diversity Combining Scheme. The performance level for the use of 2,3, and 4 antennas at the handsets can be analyzed from the figure. It can be easily concluded that the probability of error decreases with the increase in the number of antenna elements.
- Figure 4.11 depicts that when selective maximum diversity combining scheme is applied to the channel, the performance of the channel improves with the increase in the number of antenna elements. But when compared to EGC, EGC has a better performance with the increase in no. of elements as compared to SMC.

- Even in figure 4.12, the BER improves with the increase in the no. antenna elements. Now by looking at the plots for the three diversity techniques and comparing them for BER, it can be concluded that as the no. of antenna elements increases the performance of the channel improves, and also MRC provides with the best level of performance as compared to other two diversity techniques.
- Figure 4.13 shows that the performance of the antenna system with applied EGC for Ricean fading channel. It can be inferred that as the number of antenna elements increases the performance also increases.
- Figure 4.14 depicts that when SC scheme is applied to the channel, the performance of the channel improves with the increase in the number of antenna elements. But when compared to EGC, EGC has a better performance with the increase in no. of elements as compared to SMC.
- In figure 4.15, the performance of the system improves with the increase in the no. antenna elements. The graph is plotted for MRC Ricean Fading Channel and it also depicts the same thing that the performance improves with the increase in the number of antenna elements. For the three diversity techniques applied, by comparing them for BER, it can be concluded that as the no. of antenna elements increases the performance of the channel improves, and also MRC provides with the best level of performance as compared to other two diversity techniques
- Figure 4.15, it can be concluded that the level of performance for the antenna system improves with the increase in the number of antenna elements. Also with increasing SNR, probability of error decreases.
- Figures 4.16, it can be easily concluded that the performance improves with the increase in the no. of elements
- From figure 4.17 it is inferred that the BER decrease with increase in the number of antenna elements. Also by comparing the three diversity techniques for Nakagami Channel, it can be concluded that out of the three diversity techniques applied, MRC still provides the highest level of performance as compared to the other two techniques.

Table 4.1 Comparison of BER for 1-path and 2-order diversity combiner Rayleigh Fading Channel

Table 4.2 Comparison of BER for 1-path and 2-order diversity combiner

SNR (dB)	Bit Error Rate			
	1-path Rayleigh Fading Channel	2-path Rayleigh Fading Channel with applied Diversity combiner		
		Equal Gain	Maximal Ratio	Selective Maxima
1	0.1269	0.1057	0.0934	0.1057
5	0.0649	0.0377	0.0319	0.0377
10	0.0229	0.0072	0.0055	0.0072

Ricean Fading Channel

SNR (dB)	Bit Error Rate			
	1-path Ricean Fading Channel	2-path Ricean Fading Channel with applied Diversity combiner		
		Equal Gain	Maximal Ratio	Selective Maxima
1	0.1225	0.0502	0.0104	0.0709
5	0.0626	0.0162	0.0010	0.0389
10	0.0275	0.0037	0.0000	0.0196

Table4 .3 Comparison of BER for 1-path and 2-order diversity combiner

Nakagami Fading Channel

SNR (dB)	Bit Error Rate			
	1-path Nakagami Fading Channel	2-path Nakagami Fading Channel with applied Diversity combiner		
		Equal Gain	Maximal Ratio	Selective Maximum
1	0.1644	0.0829	0.0680	0.0832
5	0.0877	0.0260	0.0199	0.0263
10	0.0316	0.0032	0.0027	0.0035

Table 4.4 Comparison of BER for diversity combiner Rayleigh Fading Channel for different no. of antenna elements

No. of Antenna Elements	SNR (dB)	Bit Error Rate		
		EGC	MRC	SMC
2	1	0.1061	0.0934	0.1065
	5	0.0387	0.0312	0.0389
	10	0.0068	0.0054	0.0068
3	1	0.0626	0.0499	0.0687
	5	0.0153	0.0097	0.0185
	10	0.0013	0.0007	0.0016
4	1	0.0381	0.0276	0.0504
	5	0.0062	0.0037	0.0104
	10	0.0002	0.0001	0.0005

Table 4.5 Comparison of BER for diversity combiner Ricean Fading Channel for different no. of antenna elements

No. of Antenna Elements	SNR (dB)	Bit Error Rate		
		EGC	MRC	SMC
2	1	0.0494	0.0099	0.0718
	5	0.0152	0.0009	0.0381
	10	0.0034	0.0000	0.0203
3	1	0.0216	0.0038	0.0544
	5	0.0041	0.0002	0.0319
	10	0.0005	0.0000	0.0179
4	1	0.0102	0.0017	0.0446
	5	0.0013	0.0000	0.0277
	10	0.0001	0.0000	0.0166

Table 4.6 Comparison of BER for diversity combiner Nakagami Fading Channel for different no. of antenna elements

No. of		Bit Error Rate
--------	--	----------------

Antenna Elements	SNR (dB)	EGC	MRC	SMC
2	1	0.0831	0.0678	0.0834
	5	0.0269	0.0207	0.0270
	10	0.0038	0.0028	0.0040
3	1	0.0449	0.0315	0.0498
	5	0.0089	0.0055	0.0111
	10	0.0005	0.0004	0.0007
4	1	0.0254	0.0156	0.0346
	5	0.0030	0.0016	0.0050
	10	0.0001	0.0001	0.0002

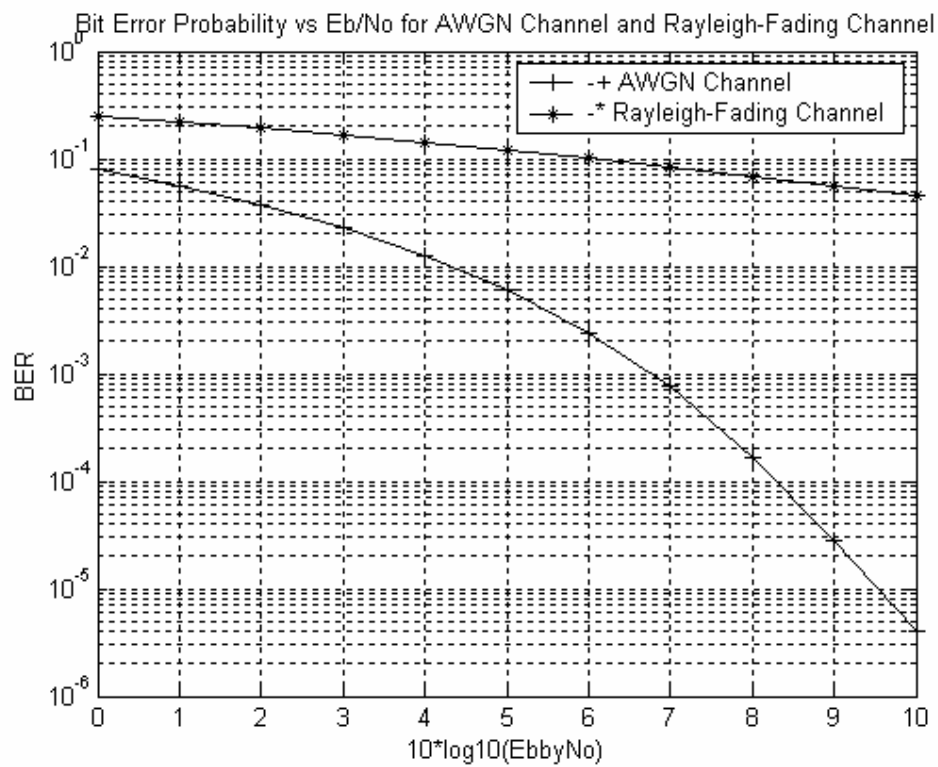


Fig. 4.3 Plot of the Bit Error Probability vs. SNR for AWGN and Rayleigh Fading Channel

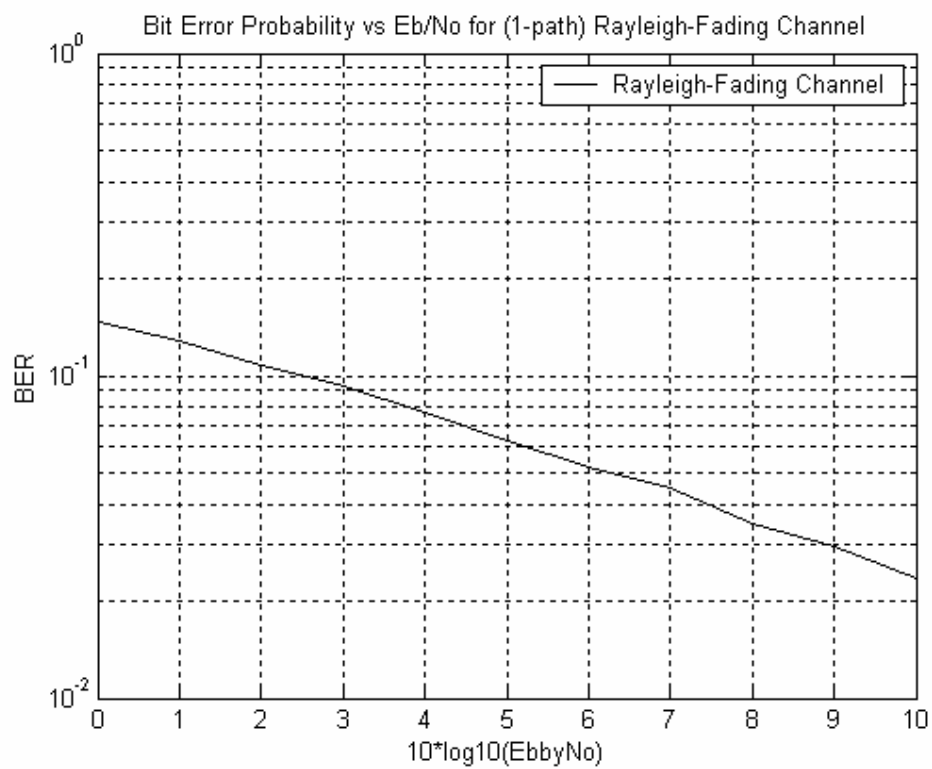


Fig. 4.4 Plot of BER vs. Eb/No for 1-path Rayleigh Fading Channel

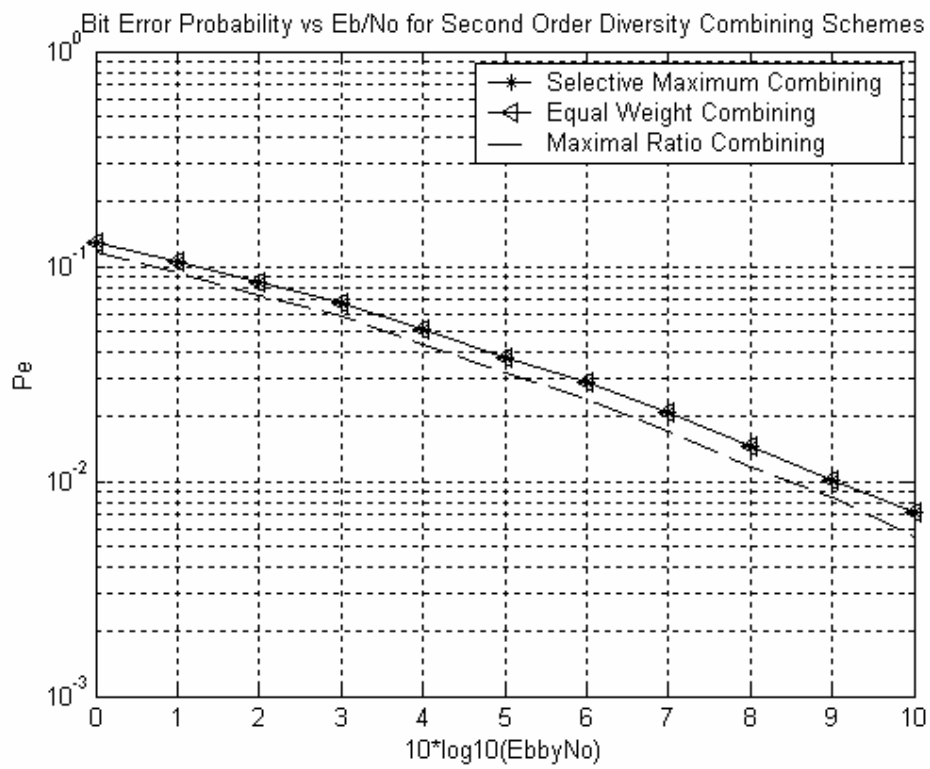


Fig. 4.5 Plot of BER vs Eb/No for Rayleigh Fading Channel using Second Order Diversity Combining Schemes

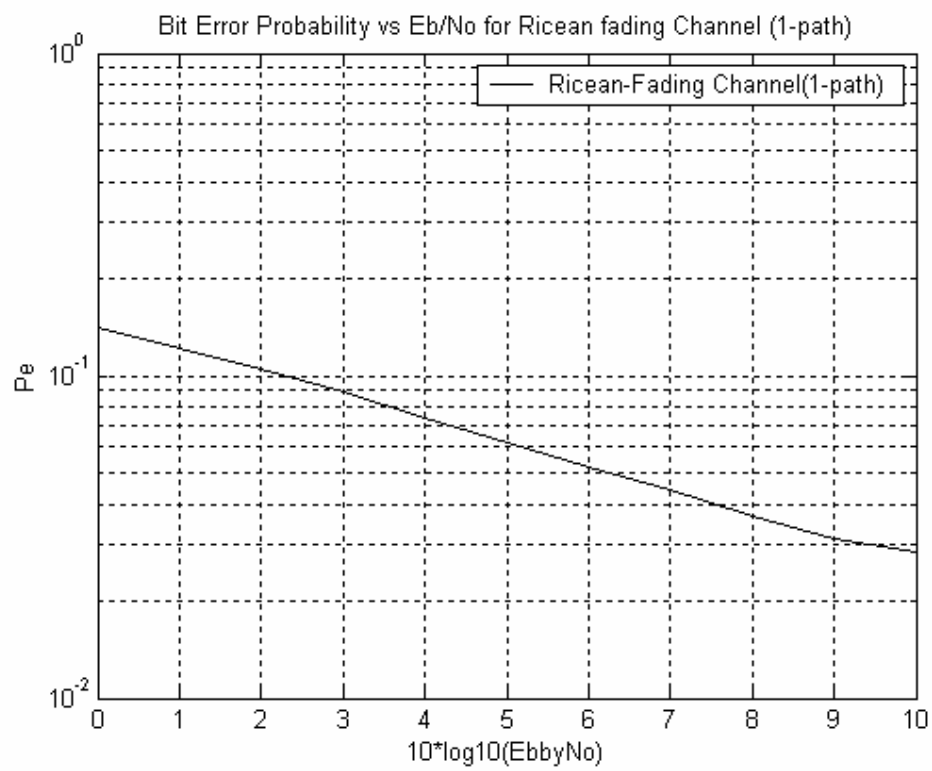


Fig. 4.6 Plot of BER vs. Eb/No for 1-path Ricean Fading Channel

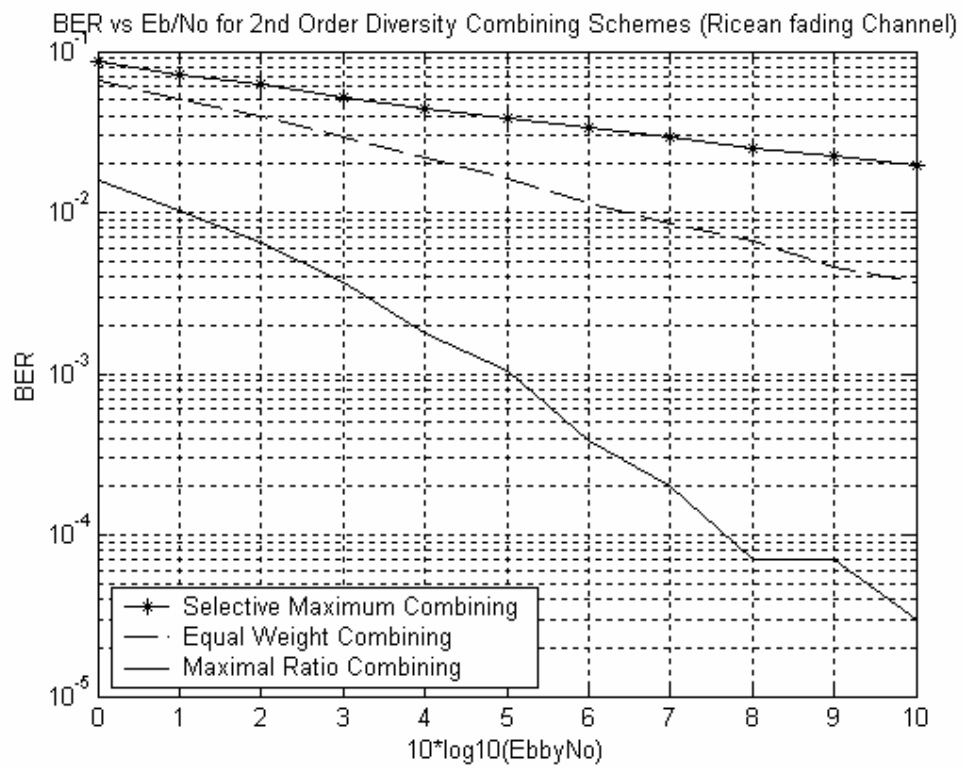


Fig. 4.7 Plot of BER vs. Eb/No for Rician Fading Channel using Second Order Diversity Combining Schemes

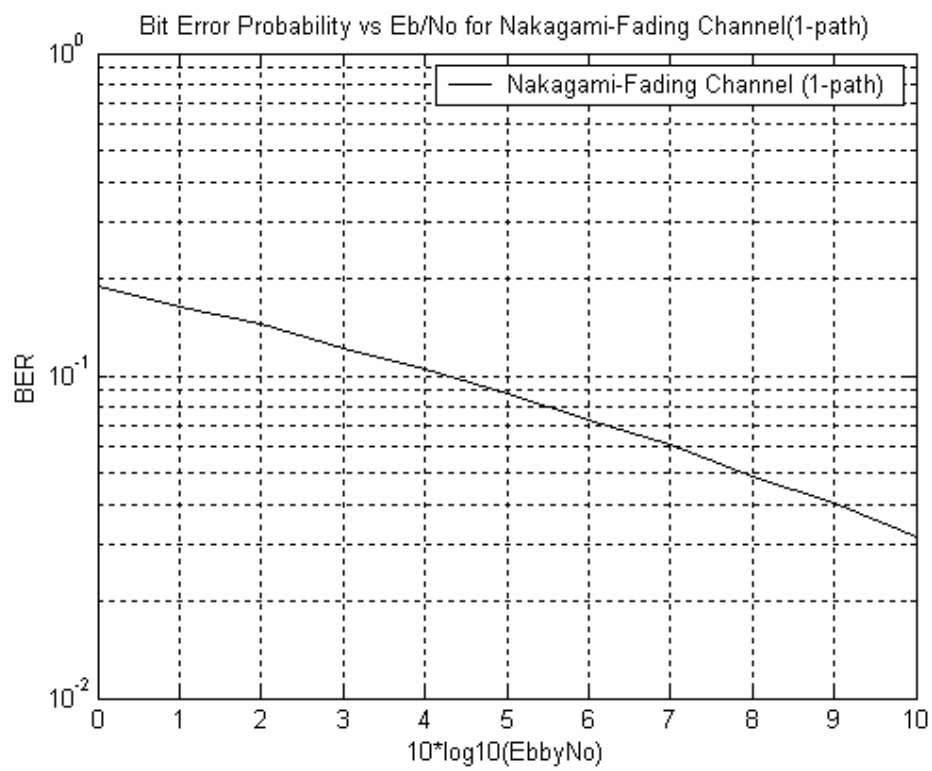


Fig. 4.8 Plot of BER vs. Eb/No for 1-path Nakagami Fading Channel

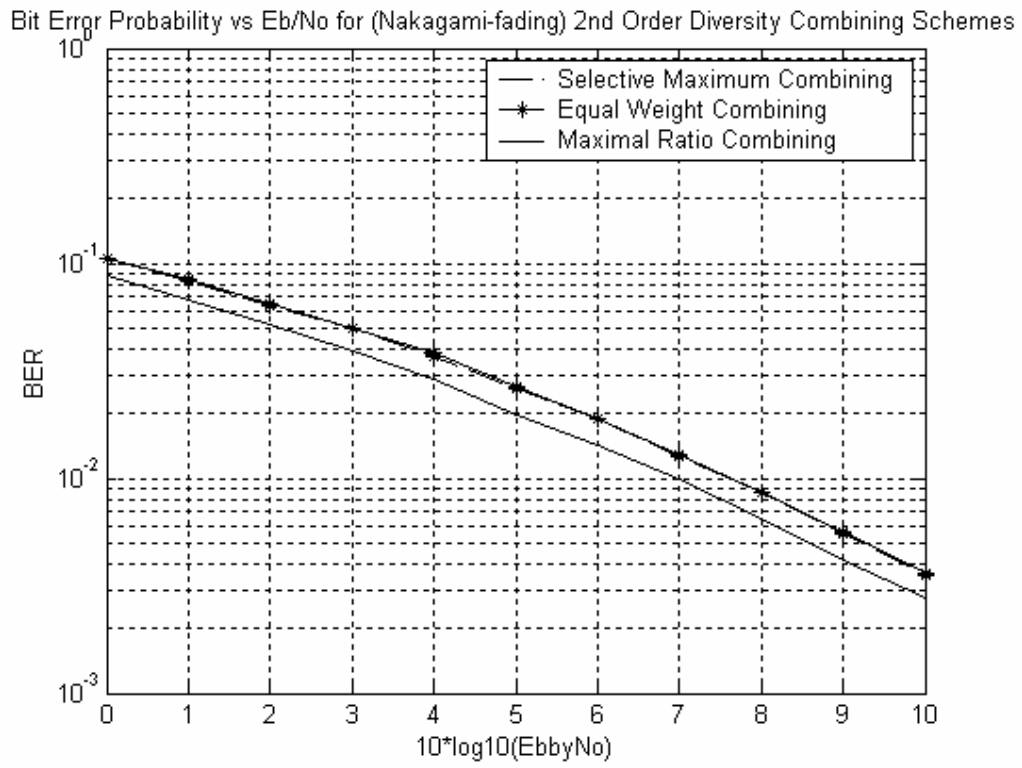


Fig. 4.9 Plot of BER vs. Eb/No for Nakagami Fading Channel using Second Order Diversity Combining Schemes

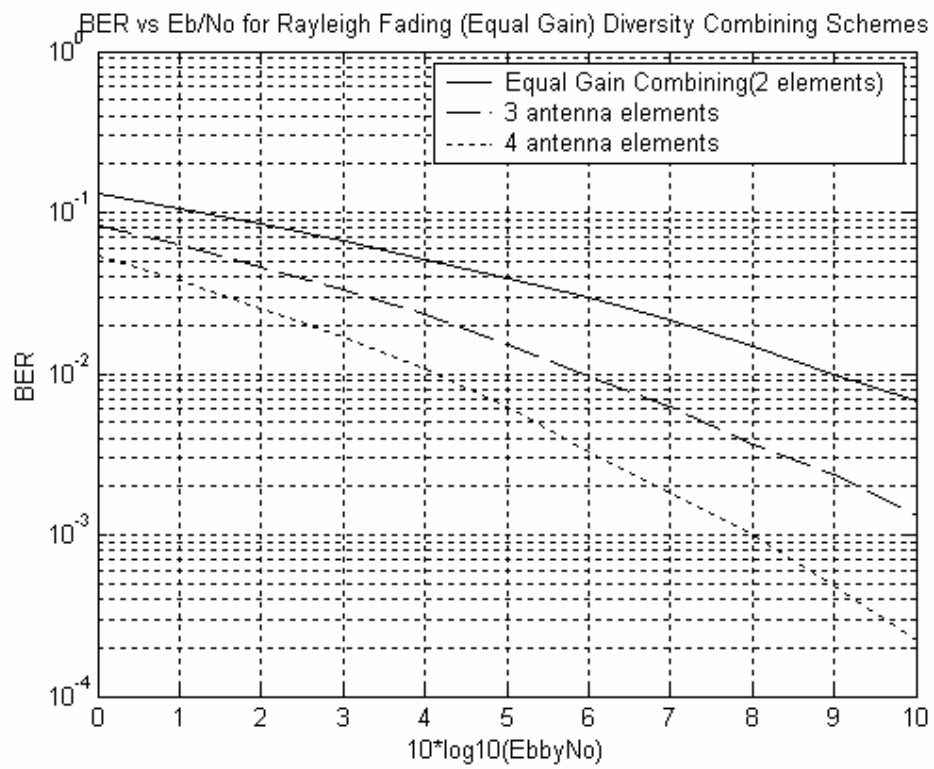


Fig. 4.10 Plot of BER vs. E_b/N_0 for Rayleigh Fading Channel with the increase in no. of antenna elements using Equal Gain Diversity Combining

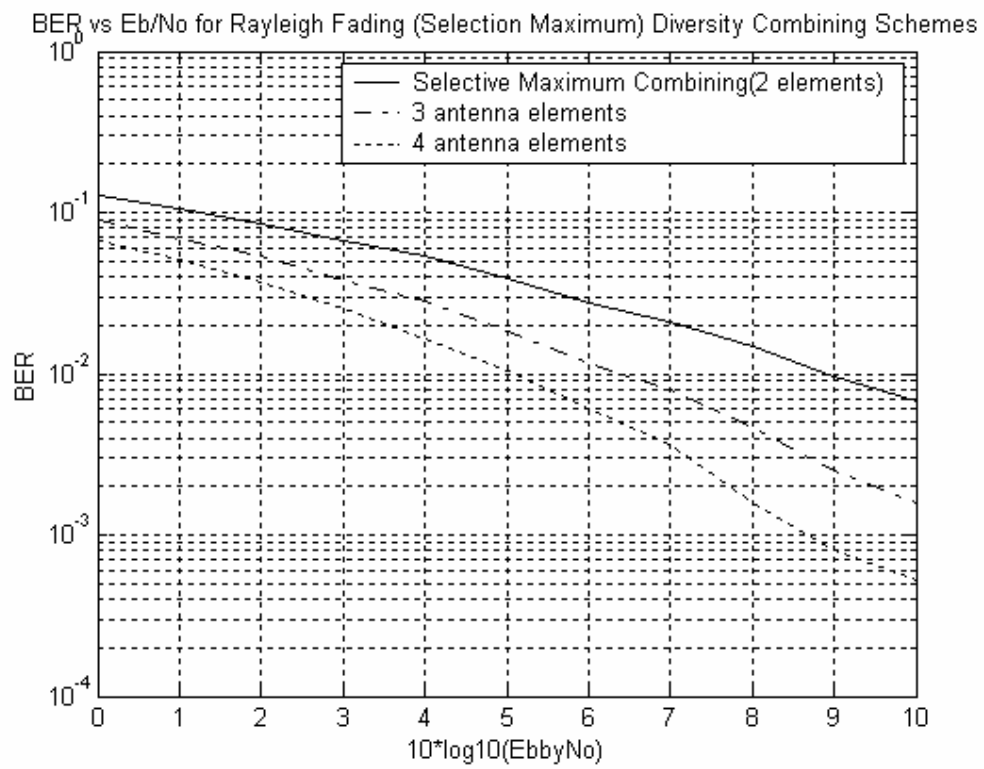


Fig. 4.11 Plot of BER vs. Eb/No for Rayleigh Fading Channel with the increase in no. of antenna elements using Selective Maximum Diversity Combining

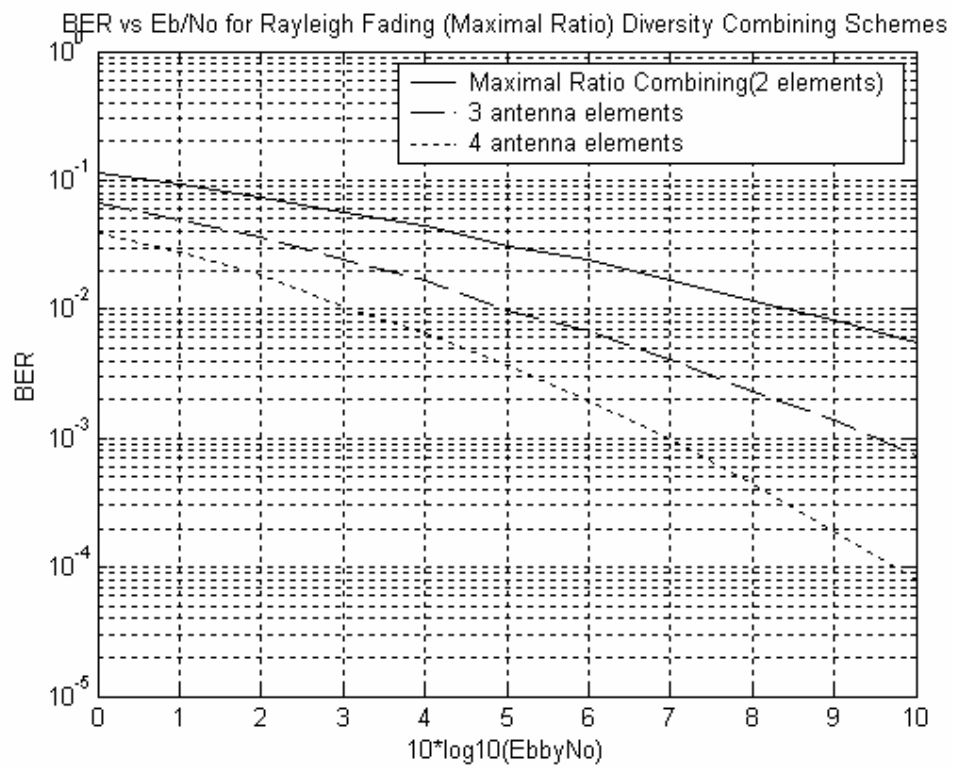


Fig. 4.12 Plot of BER vs. Eb/No for Rayleigh Fading Channel with the increase in no. of antenna elements using Maximal Ratio Diversity Combining

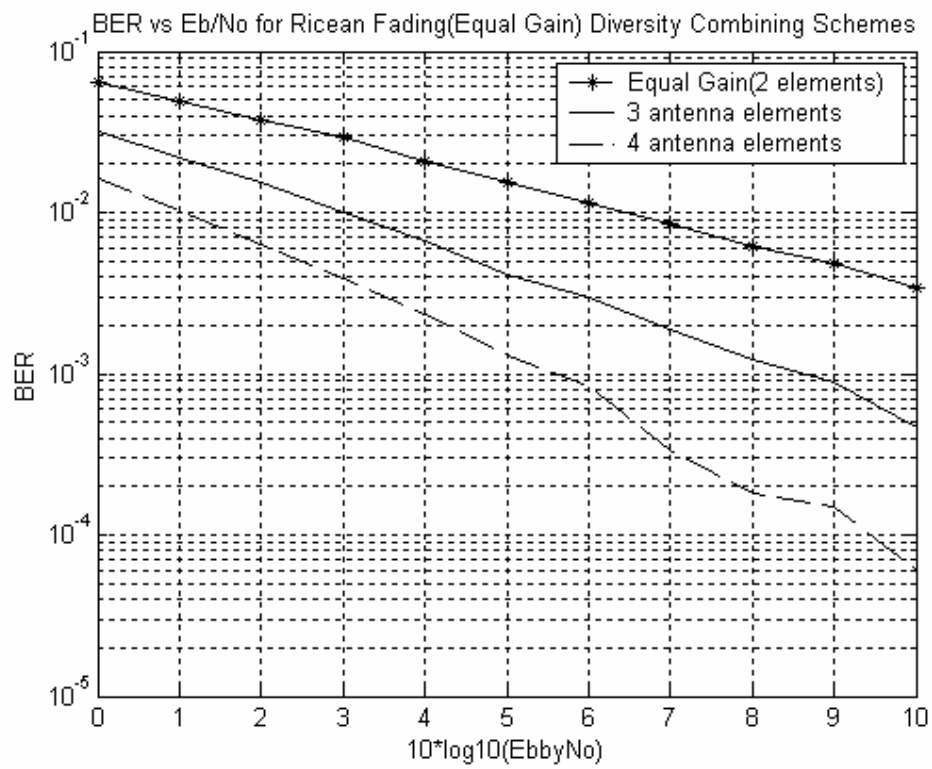


Fig. 4.13 Plot of BER vs. Eb/No for Ricean Fading Channel with the increase in the no. of antenna elements using Equal Gain Diversity Combining

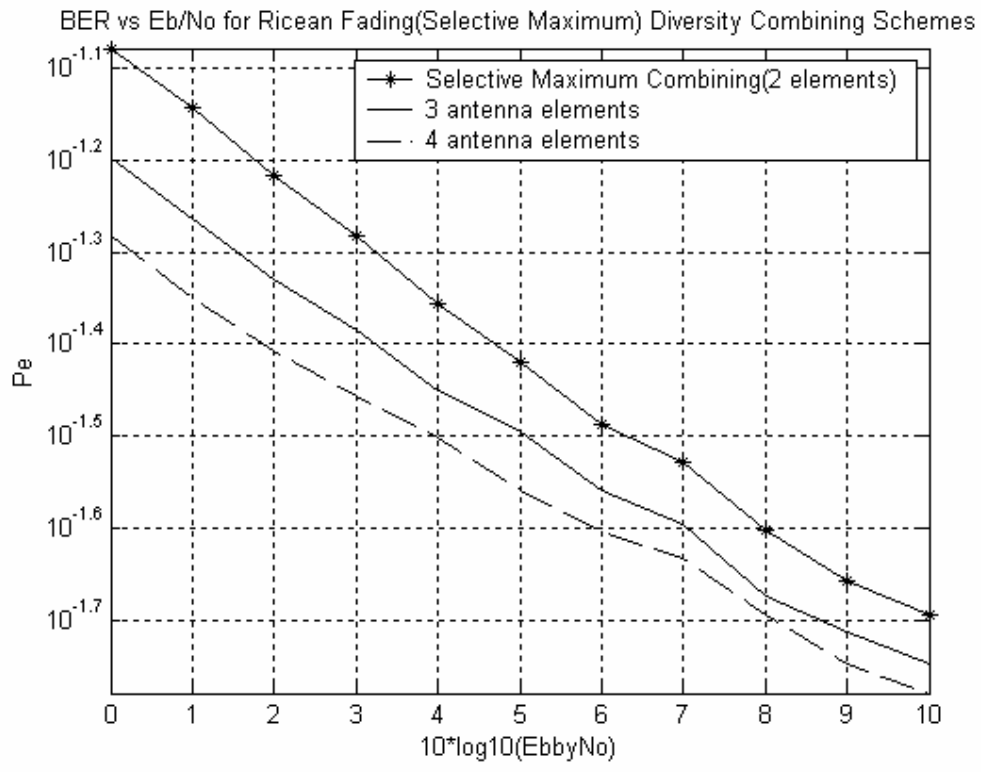


Fig. 4.14 Plot of BER vs. E_b/N_0 for Ricean Fading Channel with the increase in the no. of antenna elements using Selective Maximum Diversity Combining

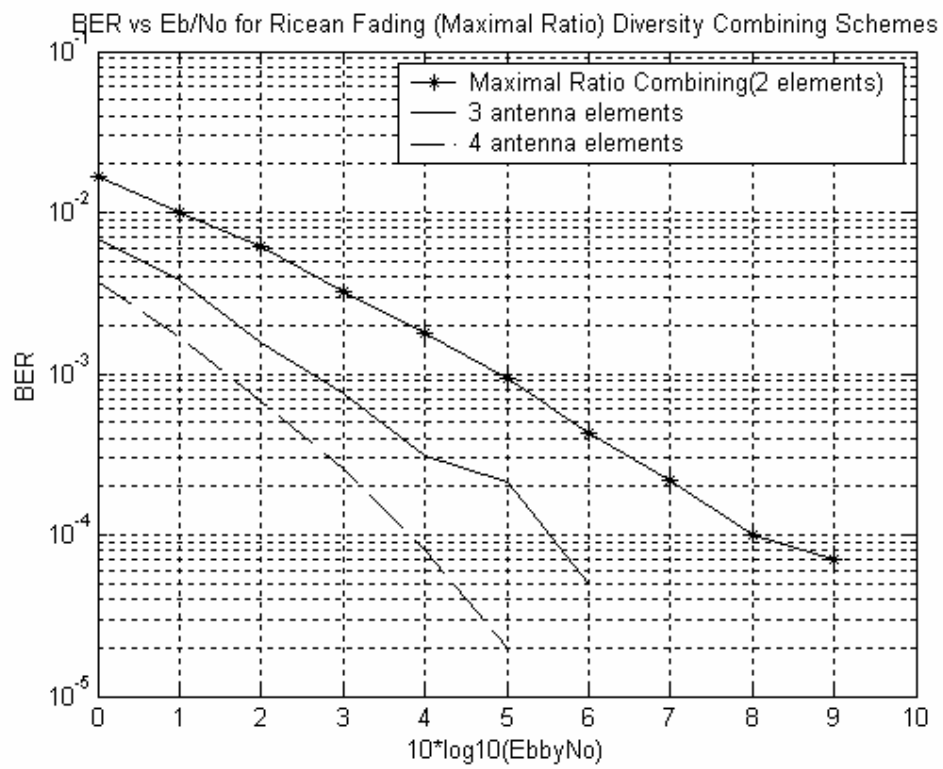


Fig. 4.15 Plot of BER vs. E_b/N_0 for Ricean Fading Channel with the increase in the no. of antenna elements using Maximal Ratio Diversity Combining

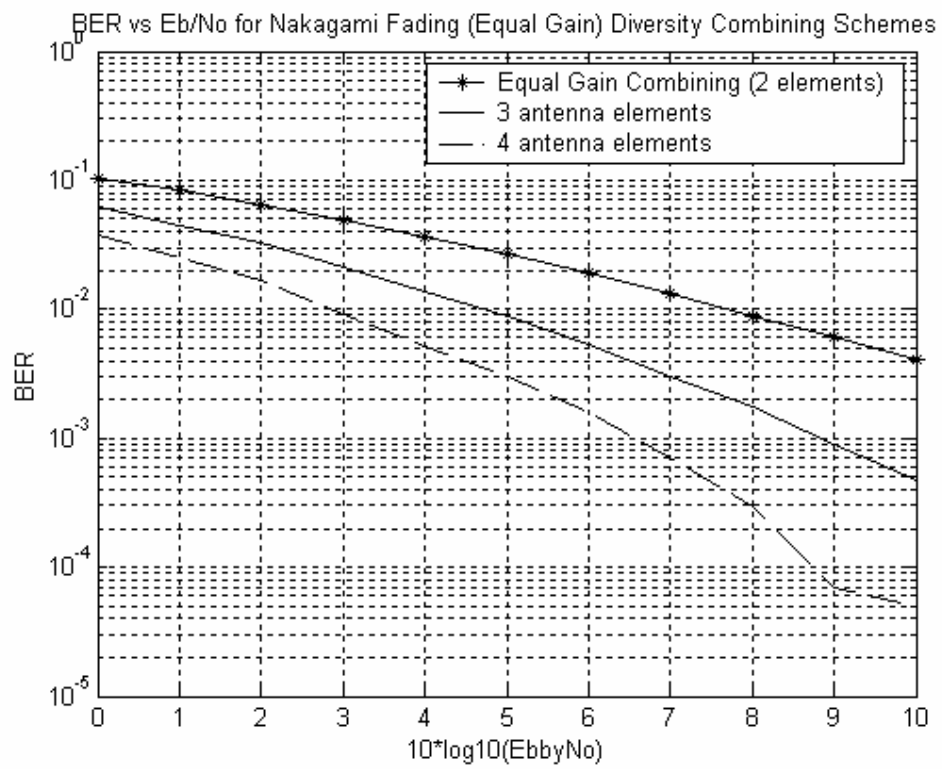


Fig. 4.16 Plot of BER vs. Eb/No for Nakagami Fading Channel with the increase in the no. of antenna elements using Equal Gain Diversity Combining

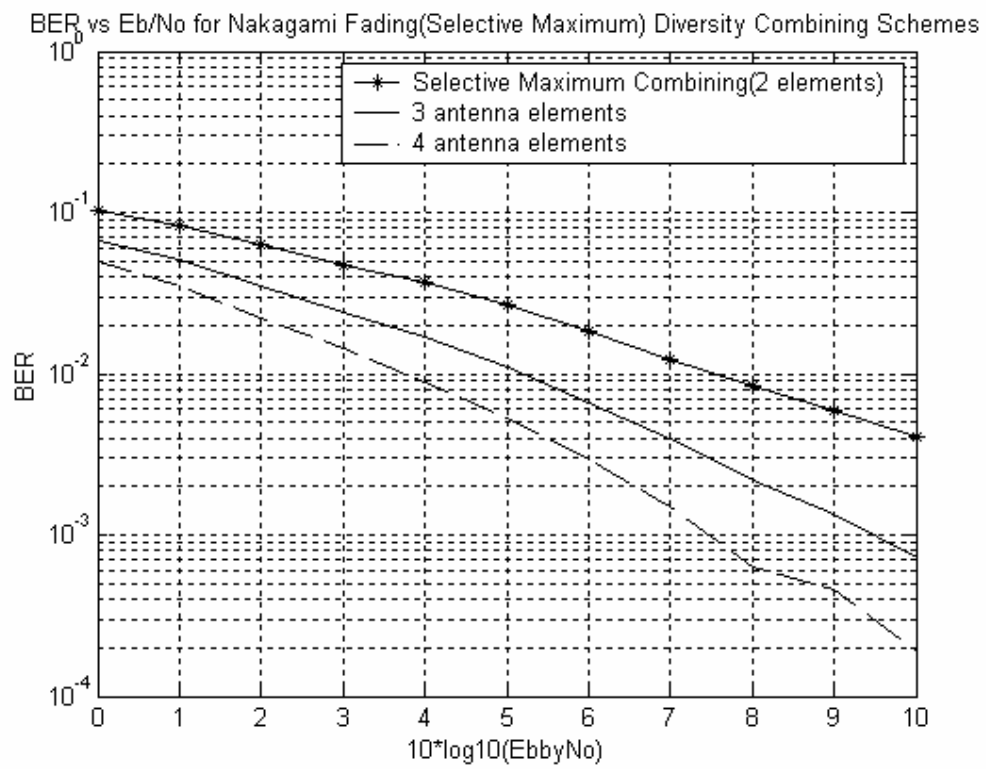


Fig. 4.17 Plot of BER vs. Eb/No for Nakagami Fading Channel with the increase in the no. of antenna elements using Selective Maximum Diversity Combining

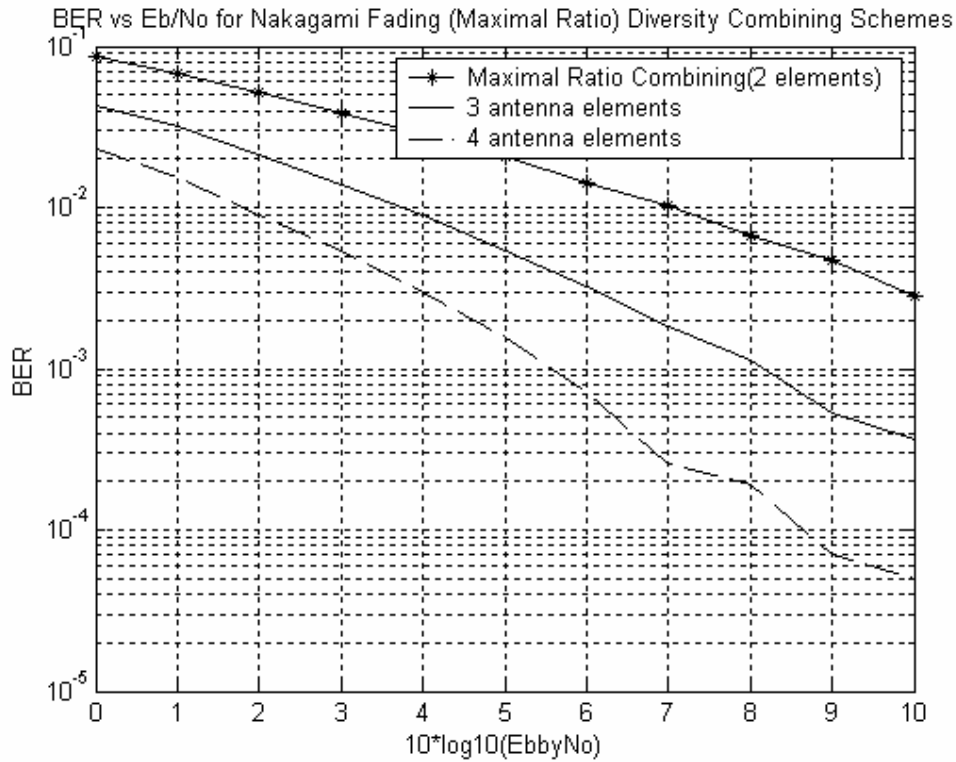


Fig. 4.18 Plot of BER vs. Eb/No for Nakagami Fading Channel with the increase in the no. of antenna elements using Maximal Ratio Diversity Combining

Chapter-5

Spatio-temporal Channel Models

In this chapter spatial channel models are discussed in detail. These models are more realistic in a sense that they give information about the amplitude, phase, and AOA of multipath delay spreads. The multipath propagation environment required by these models is also mentioned. The advantages and disadvantages of these channels are also discussed in brief. Under these channels, the two main models are the GBSB Elliptical and the GBSB Circular, which are detailed including their geometry and the mathematical assumptions.

Finally, the analysis of these channels for 1-path models, for applied diversity techniques, and for variation in number of antenna elements is shown.

5.1 Overview

As communication systems have progressively increased in complexity, many new methods have been investigated for increasing performance and capacity. There are many applications that have arisen requiring more in depth information about the propagation of electromagnetic waves. Smart antennas and systems used in position location are among the most popular new studies that require signal information such as the amplitude, phase, and AOA of multipath delay spreads. For proper and efficient implementation of future systems, emerging wireless systems must be able to exploit processing of spatial information. Antenna array systems and RAKE receivers have the ability to recombine the information from multipath components of signals allowing detection with lower bit error rates while using lower transmit power. However, the design of these systems depends heavily on information about the typical channel response. As a result, the research and implementation of AOA models, discussed in this chapter, has been motivated by a real world need for this type of data.

5.2 Multipath Propagation Environment

Antenna arrays are often used to mitigate the effect of fading and thereby increasing the system capacity. Antenna array is also used for diversity combining. Base don the fact that spatio channel model is required to test the performance of antenna array same models have been used in analyzing performance of diversity techniques. Application of antenna arrays may range from fixed directional spatial-filtering to adaptive beamforming. To test the performance of antenna arrays, an accurate description of the spatio-temporal channel model is required [13].

It is first useful to, once again, illustrate how a transmitted signal interacts with the environment. When electromagnetic waves are transmitted, reflections from large objects, diffraction of the waves around objects, and signal scattering dominate the received signal resulting in the presence of multipath components, or *multipath* signals, at the receiver. Figure 5.1 depicts a general example of this multipath environment. Each signal component propagates through a different path, determining the amplitude $A_{l,k}$, carrier phase shift $\varphi_{l,k}$, time delay $\tau_{l,k}$, angle of arrival $\theta_{l,k}$, and Doppler shift f_d of the l th signal component of the k th mobile. Accordingly, each of these signal parameters will be time-varying [14].

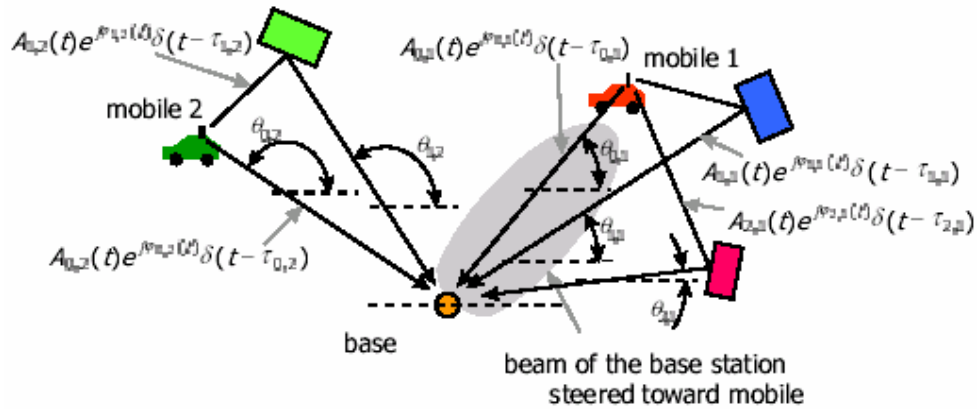


Fig. 5.1 The Simplified Multipath Environment

The vector channel impulse response characterizing Figure 5.1 can be expressed as in Equation (5.1), where $\vec{a}(\theta_l(t))$ is the *array response vector*. Equation (5.1) is the spatial channel impulse response for the first mobile user and is made up of the summation of several multipath components, each having its own amplitude, phase, and angle-of-arrival where $L(t)$ is the number of multipath components .

$$\vec{h}_1(t, \tau) = \sum_{l=0}^{L(t)-1} A_{l,1}(t) e^{j\phi_l(t)} \vec{a}(\theta_l(t)) \delta(t - \tau_l(t)) \quad (5.1)$$

When antenna arrays are employed, the array response vector is a function of the antenna array geometry and the AOA. This vector normally is described as in Equation (5.2),

$$a(\theta_l(t)) = \begin{bmatrix} \exp(-j\psi_{l,1}) \\ \exp(-j\psi_{l,2}) \\ \dots \\ \exp(-j\psi_{l,m}) \end{bmatrix} \quad (5.2)$$

where

$$\psi_{l,i}(t) = [x_i \cos(\theta_l(t)) + y_i \sin(\theta_l(t))] \beta, \quad \text{and}$$

$\beta = 2\pi / \lambda$ is the wave number. The variable, m , defines the number of elements and (x_i, y_i) , is the coordinate of the i -th element. The distribution of these parameters given in Equation (5.2) is dependent upon the type of environment. More specifically, research has shown that the angle spread of the channel is a function of both the environment and the base station antenna heights. This research has led to the development of spatial models for many different applications.

Classically, the rich scattering multipath environment is modeled as the Rayleigh fading phenomena. In this model, it is assumed that the signals are arriving uniformly along the azimuthal direction. However in more realistic scenarios, the AOA of the multipath depends on a number of factors, such as the distance between the transmitter and receiver, location of scatterers, size of the receiving antenna etc. A number of channel models have been proposed in the literature based on both measurement data and statistical properties of the channel. Some of these models are suited to the microcells typically set up in urban areas, while others are more applicable for the macrocells found in the rural and suburban areas. There are also channel models based on propagation statistics in the indoor environment. All these models provide multipath parameters including the AOA information essential to simulate an antenna array system.

In this chapter, two spatial channel models known as GBSB Elliptical and GBSB Circular are described for micro and macro-cellular environments [20]. In these models it is assumed that the multipath reflections are created by random placement of scatterers inside a region defined by a specific geometry. From the position of the scatterers, multipath delays, AOA and power levels are determined. Thus these models provide a statistical description of the wideband spatio-temporal radio channel, which is useful in simulating a space-time processing system. The chapter is organized as follows: Section 5.3 gives a brief description of the GBSB elliptical channel model and the method of generating the channel parameters for simulation purpose. Section 5.4 describes the GBSB circular channel model in a similar fashion.

5.3 Advantages and disadvantages of GBSB models

5.3.1 Disadvantages

The expected power delay profiles for the GBSB channel models are determined by the concentration of objects on concentric ellipses, defined such that the transmitter and receiver are placed at foci. Each ellipse corresponds to a particular delay. Therefore, it is possible to predict the power delay profile simply from the geometry of the model. In general the geometrical based vector channel models do not provide much flexibility in the independent selection of the channel parameters. Furthermore, some of the models are only appropriate for specific environments. When simulating different environments different channel model structures may be needed. This lack of flexibility inherent in the geometrical models is the major disadvantage of using such a model [20].

5.3.2 Advantages

An advantage of the geometrical models is that they provide the complete specification of the joint AOA/TOA statistics of the channel in a very compact form. For

example, simply specifying that scatterers be uniformly distributed within a circular region about the mobile of radius 20m is all that is needed to specify the spatial aspects of the channel. Additionally, many of the models seamlessly adjust to different T-R separation distance. For example, with the circular model, the angle spread will automatically decrease with an increase in the T-R separation as desired.

Another potential advantage of these models is that by placing objects in space the resulting channel at least in some sense is modeling a physical property of the real world. However, the actual phenomena which is occurring is extremely difficult to characterize, and hence using a highly idealized physical model of the channel may not give an accurate representation of what is actually happening. In this case, it may be best to consider the statistical characterization of measurement data rather than attempt to model the physical mechanism behind the data.

5.4 Geometrically Based Single Bounce Elliptical Model

In a typical urban environment dense scattering coupled with abundance of reflection results in a rich multipath scenario. In this situation, the micro cellular concept where the base station has a relatively low antenna height is more appropriate. This implies that the multipath scatterers are located near the base station as well as near the mobile. Therefore, any spatial channel model that employs a geometrical scattering region around the mobile must also consider a similar scattering region around the base station. A particular channel model, which uses an elliptical scattering region surrounding the base station and the mobile, has been proposed for the microcell environment. This GBSB elliptical channel model is chosen for this research to describe a typical urban multipath propagation scenario [3].

5.4.1 Assumptions

The following assumptions are made in developing the elliptical channel model .

- The signals arriving at the base station are plane waves propagating along the horizon. As a consequence the AOA is calculated only in the azimuthal coordinates.
- The scatterers are omni-directional re-radiating elements having identical scattering coefficients.
- All scatterers are uncoupled. In other words, the signals reflected from each scatterer are not affected by the presence of the other scatterers.
- The received multipath signals are subjected to distance-dependent path loss characterized by a path loss exponent.

5.4.2 Geometry and Notation

In the GBSB elliptical channel model the scatterers are assumed to be uniformly distributed in an elliptical region. The base station and the mobile form the foci of the ellipse. The geometry of the elliptical model is shown in Figure 5.2.

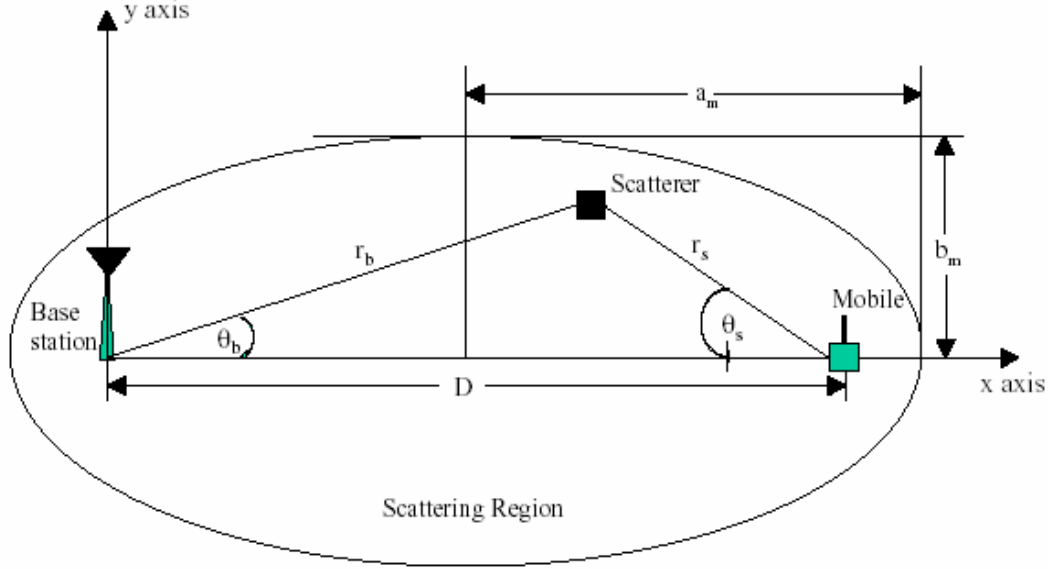


Figure 5.2 Geometry of the GBSB elliptical channel model

In Figure 5.2, a distance D separates the base station and the mobile, with the base station at the origin. All scatterers lie in a plane that includes the base station and the mobile, implying that the reflected multipath waves will appear to have the same elevation angle. The elliptical region is completely described by its semi-major axis, a_m and its semi-minor axis, b_m . The choice of these parameters is determined by the maximum delay, τ_{\max} of the multipath. Larger values of τ_{\max} imply greater path loss for the multipath and, consequently, lower relative power compared to those with shorter delays. Hence, this model has a nice physical interpretation in that, changing the geometry of the ellipse can automatically adjust the various channel parameters, such as multipath amplitudes, delay spread and angle spread.

5.4.3 Mathematical Formulation

The semi-major axis, a_m and its semi-minor axis, b_m are related to the maximum specified delay τ_{\max} as below

$$a_m = \frac{c\tau_{\max}}{2}, \quad b_m = \frac{1}{2}\sqrt{c^2\tau_{\max}^2 - D^2} \quad (5.3)$$

where, D is the separation distance between the transmitter and the receiver and c is the speed of propagation (3×10^8 m/s). The equation of an ellipse in Cartesian coordinates

$$\begin{aligned} \frac{(x - D/2)^2}{a_m^2} + \frac{(y)^2}{b_m^2} &= 1 \\ \Rightarrow \frac{(x - D/2)^2}{\left(\frac{c\tau_{\max}}{2}\right)^2} + \frac{y^2}{\left(\frac{\sqrt{c^2\tau_{\max}^2 - D^2}}{2}\right)^2} &= 1 \end{aligned} \quad (5.4)$$

Substituting, $x = r_b \cos(\theta_b)$ and $y = r_b \sin(\theta_b)$, the equation of the ellipse in Polar coordinates

$$\frac{(r_b \cos \theta_b - D/2)^2}{\left(\frac{c\tau_{\max}}{2}\right)^2} + \frac{(r_b \sin \theta_b)^2}{\left(\frac{c^2\tau_{\max}^2 - D^2}{2}\right)^2} = 1 \quad (5.5)$$

where r_b is the distance from the base station of a scatterers located at the boundary of the ellipse and θ_b is the AOA at the base station. Any scatterers inside the ellipse can be viewed as an equivalent one located at the boundary of a smaller concentric ellipse. Equation (5.5) can then be solved for r_b for different values of the multipath propagation delay, $\tau \in [\tau_{\min}, \tau_{\max}]$. However an easier way is to utilize the coordinate location of the scatterers. Referring to Figure 5.2, the total propagation distance of a multipath ray from the mobile to the base-station

$$\begin{aligned} d &= r_b + r_s \\ &= r_b + \sqrt{(D - r_b \cos(\theta_b))^2 + (r_b \cos(\theta_b))^2} \\ &= r_b + \sqrt{D^2 + r_b^2 - 2Dr_b \cos(\theta_b)} \end{aligned} \quad (5.6)$$

Substituting $d = \tau c$ in (5.6) and solving for r_b yields

$$r_b = \frac{D^2 - \tau^2 c^2}{2(D \cos(\theta_b) - \tau c)}; \quad \frac{D}{c} \leq \tau \leq \tau_m \quad (5.7)$$

Due to the symmetric nature of the scattering region, similar expressions can be derived with respect to the mobile. A detailed analysis on the pdf of multipath delays, AOA and power spectrum of the elliptical channel model can be found in.

5.4.4 Generation of Samples of the Elliptical Channel Model

The elliptical model described above can be used to generate various multipath signal parameters such as multipath delay τ_i , AOA θ_i , and power P_i of the i^{th} multipath component. Usually there are two ways to generate these parameters. In one method, the geometrical definition of the elliptical scattering region can be utilized to calculate the parameters. In the other method, the delay and AOA statistics are used to generate the channel samples. The first method is more computationally efficient and it will be described below in detail. The idea is first to define an ellipse corresponding to the maximum multipath delay, τ_m and uniformly place the scatterer inside the ellipse. The relevant signal parameters can then be calculated from the coordinates of the scatterers. It is assumed that the number of multipaths (scatterers), L and the transmitter to receiver separation distance, D is known.

The procedure is outlined below

- A value of the maximum multipath propagation delay, τ_m is chosen
- Samples of two uniformly distributed random variables, x_l and y_l , $l=1,2,\dots,L$ are generated over the interval $[-1,1]$.
- Isolated the points that lie on and within a circle of unit radius centered at the origin. Translate them from the cartesian coordinates (x_l, y_l) to the polar coordinates (r_l, θ_l) according to the following relationships

$$r_l = \sqrt{x_l^2 + y_l^2}, \quad \phi_l = \tan^{-1}\left(\frac{y_l}{x_l}\right); \quad l = 1, 2, \dots, L \quad (5.8)$$

- Thus, L samples of a random variable described by the polar coordinates (r_l, θ_l) are obtained that are uniformly distributed in a circle of unit radius. These samples are translated so that they are uniformly distributed in an ellipse, the following two transformations are performed

$$x_l = a_m r_l \cos(\theta_l) + \frac{D}{2}, \quad y_l = b_m r_l \sin(\theta_l); \quad l = 1, 2, \dots, L \quad (5.9)$$

where, a_m and b_m are the semimajor and the semiminor axes of the ellipse respectively corresponding to the specified τ_m and are given by (5.3). The multipath propagation distance, d_l ; $l=1,2,\dots,L$ can be calculated as

$$d_l = \sqrt{x_l^2 + y_l^2} + \sqrt{(D - x_l)^2 + y_l^2}; \quad l = 1, 2, \dots, L \quad (5.10)$$

- The propagation delays of the multipaths, τ_l ; $l=1,2,\dots,L$ will be

$$\tau_l = \frac{d_l}{c}; \quad l = 1, 2, \dots, L; \quad c = 3 \times 10^8 \text{ m/s} \quad (5.11)$$

- Following that the base station is located at the origin of the coordinate system, the angle of arrivals (AOA) of the multipaths at the base station are given by

$$\theta_{b,l} = \tan^{-1} \left(\frac{y_l}{x_l} \right); \quad l = 1, 2, \dots, L \quad (5.12)$$

- The power of the direct path component (LOS) can be calculated as below

$$P_0(dBm) = P_{ref}(dBm) - 10n \log \left(\frac{D/C}{d_{ref}} \right) + G_t(\theta_d) + G_r(\theta_a) \quad (5.13)$$

where P_{ref} is the reference power measured at a distance d_{ref} from the transmitter using omni-directional antennas at the transmitter and the receiver. P_{ref} can be calculated using Friis' free space propagation model given by

$$P_{ref}(dBm) = P_T(dBm) - 20 \log \left(\frac{4\pi d_{ref}}{\lambda} \right) \quad (5.14)$$

where P_T is the transmitted power and $\lambda = c/f$ is the wavelength for a particular carrier frequency, f . The path loss exponent, n typically ranges from 3 to 4 in a microcell environment. $G_t(\theta_d)$ and $G_r(\theta_a)$ are the gains of the transmit and the receive antennas as functions of the angle of departure, θ_d and the angle of arrival, θ_a respectively. For the LOS component, θ_d and θ_a are both zero. The power of each of the multipath component can be calculated as below

$$P_l(dB) = P_o(dB) - 10n \log(d_l) - L_r + G_t(\theta_{d,l}) - G_t(0) + G_r(\theta_{a,l}) - G_r(0) \quad (5.15)$$

where L_r is the path loss in dB

- Assuming the phase of the multipath components, γ_l ; $l=1, 2, \dots, L$ are uniformly distributed over the interval $(0, 2\pi)$, the complex amplitudes of the multipath components are calculated as below

$$\alpha_l = 10^{(P_l - P_0)/20} e^{j\gamma_l}; \quad l = 1, 2, \dots, L \quad (5.16)$$

5.5 Geometrically Based Single Bounce Circular Model

A typical rural or suburban environment is characterized by local scatterers surrounding the mobile and no large reflectors away from the vicinity of the mobile is visible at the base station. In such environments, macrocellular concept where the base station antenna height is considered to be above the local clutter is a more appropriate selection. Thus, the multipath channel parameters in the propagation model for rural or suburban environment are essentially determined by the distribution of the scatterers around the mobile. A number of models have been proposed in the literature that defines the geometry and the underlying distribution of the scatterer region. In one of these models, it is assumed that the scatterers are uniformly distributed within a circle of predefined radius

around the mobile. This model known as GBSB Circular model is specially suited for macrocell environments and thus sufficient to represent a rural or suburban multipath propagation model.

5.5.1 Assumptions

A GBSB Circular model presupposes the following underlying assumptions.

- The signals received at the base station are plane waves propagating along the horizon. Thus only the azimuthal coordinates are required to represent the corresponding AOA. This is due to the fact that the separation distance between transmitter and receiver is large compared to the respective antenna heights.
- The scatterers are considered to be omni-directional re-radiating elements with identical scattering coefficients.
- Each multipath component at the base station has interacted with only a single scatterer and thus is not influenced by the other scatterers in the channel.

5.5.2 Geometry and Notation

The GBSB circular model assumes that the scatterers are uniformly distributed within a circle of radius, R around the mobile. The geometry of the circular model is shown in Figure 5.3.

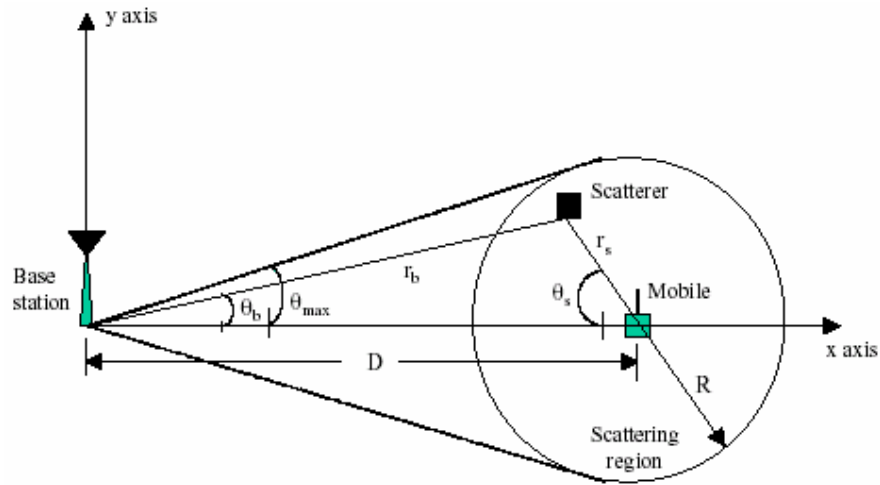


Figure 5.3 Geometry of the Circular Scattering Channel Model

In Figure 5.3, the base station and the mobile are separated by a distance D , with the base station at the origin of the coordinate system and the mobile is on the x-axis. The scatterers are uniformly placed in a circle of radius R with the mobile is at the center. Typically, $R < D$, so that there are no scatterers local to the base station as is the case in a

macrocell region. For simplicity, the plane of the scatterer can be viewed as horizontal, which also includes the mobile and the base station. This will ensure that the AOA of the received signal contains only azimuthal components. The AOA of the multipath components at the base station is denoted by θ_b and depends on two parameters: the angle of departure from the mobile and the position of the scatterer. The location of the scatterer is specified by its distance from the base station, r_b , and from the mobile, r_s , respectively. Since the scatterers are confined in a circle around the mobile, the AOA at the base station, θ_b , is limited by a maximum value denoted by, θ_{\max} . Similarly, the AOA at the mobile, θ_s depends on the angle of departure from the base station and the scatterer location. In this case, as the mobile is located inside the scattering region, the AOA can be any value in the interval $[0, 2\pi)$. The radius of the circular scattering region, R , is usually determined by equating the angle spread as predicted by the model with the measured angle spread. Typical values of angle spread in a macrocell environment ranges between one to six degrees for a transmitter to receiver separation distance of $D \approx 1$ km. Using the fact that the angle spread is inversely proportional to D , the measurement results suggest a radius of scatterer ranging from 30 to 200 m.

5.5.3 Mathematical Formulation

The region of scatterer in the Cartesian coordinates is given by

$$(x - D)^2 + y^2 \leq R^2 \quad (5.17)$$

Substituting, $x = r_b \cos(\theta_b)$ and $y = r_b \sin(\theta_b)$ in (4.4.4.1) and expanding, the scattering region in Polar coordinates

$$r_b^2 - 2r_b D \cos(\theta_b) + D^2 \leq R^2 \quad (5.18)$$

Referring to Figure 5.3, the total multipath propagation distance, d is given by

$$\begin{aligned} d &= r_b + r_s \\ &= r_b + \sqrt{(D - r_b \cos(\theta_b))^2 + (r_b \sin(\theta_b))^2} \\ &= r_b + \sqrt{D^2 + r_b^2 - 2Dr_b \cos(\theta_b)} \end{aligned} \quad (5.19)$$

Substituting $d = \tau c$, where τ is the multipath propagation delay, the distance of the scatterer from the base station, r_b , can be expressed as

$$r_b = \frac{D^2 - \tau^2 c^2}{2(D \cos(\theta_b) - \tau c)}; \quad (5.20)$$

As in the GBSB elliptical channel model, the symmetric nature of the scattering region allows similar expressions to be derived with respect to the mobile.

5.5.4 Generation of Samples of the Circular Channel Model

As in the elliptical channel model, there are two ways to generate the multipath channel parameters using the circular channel model. Exploitation of the geometry of the scattering region, which will be described below, is a much more efficient method than the one that utilizes the statistics of the channel parameters (delay, AOA). Again, the basic idea is to define a uniform circular scattering surrounding the mobile with the radius corresponds to the maximum multipath delay, τ_m . The relevant signal parameters can then be calculated from the geometry of the scattering region. As in the case of elliptical model, it will be assumed that number of multipaths, L and the transmitter to receiver separation distance, D is known.

The procedure is described below [13].

- A value of the maximum multipath propagation delay, τ_m , is chosen
- The radius of the scattering region is calculated according to the following relationship

$$R_m = \frac{(c\tau_m - D)}{2} \quad (5.21)$$

where c is the speed of propagation

- Samples of two uniformly distributed random variables, x_l and y_l , $l=1,2\dots L$ are generated over the interval $[-R_m, R_m]$ and the points that lie on and inside a circle of radius R_m are isolated. The coordinates of these points to an origin at a distance D from the center of the circle is

$$x_c = x_l + D, \quad y_c = y_l; \quad l = 1,2\dots L \quad (5.22)$$

- The multipath propagation distance, d_l ; $l=1,2\dots L$ can be calculated as

$$d = \sqrt{x_c^2 + y_c^2} + \sqrt{(D - x_c)^2 + y_c^2} \quad (5.23)$$

- The propagation delays of the multipaths, τ_l and AOA at the base station (origin) $l=1,2\dots L$ are

$$\tau_l = \frac{d_l}{c}, \quad \theta_{b,l} = \tan^{-1}\left(\frac{y_c}{x_c}\right); \quad l = 1,2\dots L \quad (5.24)$$

- The power of each of the multipath component can be calculated as below

$$P_l(dB) = P_o(dB) - 10n \log(d_l) - L_r + G_t(\theta_{d,l}) - G_t(0) + G_r(\theta_{a,l}) - G_r(0) \quad (5.25)$$

where L_r is the path loss in dB

- Assuming the phase of the multipath components, γ_l ; $l=1,2,\dots,L$ are uniformly distributed over the interval $(0,2\pi)$, the complex amplitudes of the multipath components are calculated as below

$$\alpha_l = 10^{(p_l - p_0)/20} e^{j\gamma_l}; \quad l = 1, 2, \dots, L \quad (5.26)$$

5.6 Channel Description

The spatio-temporal channel models described in this Chapter provide a statistical description of the multipaths channel parameters such as channel gain, propagation delays, AOA etc. However, for the purpose of analysis, a simple parametric model represented by a summation of delta functions associated with different amplitudes, time delays and AOA is more useful. Each of these delta functions corresponds to a resolvable multipath in a frequency selective fading channel, as is the case for a W-CDMA signal. Thus the channel impulse response formed in this manner provides a mean description of the statistically distributed channel parameters in both space and time.

An important parameter that characterizes the spatial channel is the angle spread, Δ defined as the spread of the AOA of the discrete multipath components. In other words, each of the delta functions in the channel impulse response is in reality a combination of a number of delta functions (subpaths), which arrive very closely in time but may have different directions. The range of the AOA of these subpaths is characterized by the angle spread. As we will see, this parameter has an important effect on different array processing and combining techniques. As mentioned earlier, a W-CDMA system undergoes frequency selective fading when the relative multipaths delays are more than a chip period. This time dispersiveness property of the channel is characterized by the delay spread defined in a similar way as the angle spread. That is, delay spread is a measure of spread of the multipaths in time domain. The time-varying property of the channel model is defined by the Doppler spread. For the spatio-temporal channel models, an accurate description of Doppler power spectrum is still to be formulated.

Let us consider an N -element linear antenna array at the receiver. The channel impulse response of the i th user can be expressed as

$$h_i(t) = \sum_{l=1}^{L_i} \alpha_{l,i}(t) a(\theta_{l,i}) \delta(t - \tau_{l,i}) \quad (5.27)$$

where L_i is the number of resolvable multipaths from the i th user each characterized by a complex path amplitude $\alpha_{l,i}(t)$ and a path delay $\tau_{l,i}$. The $N \times 1$ array response vector or the steering vector $a(\theta_{l,i})$ is defined as

$$a(\theta_{l,i}) = \begin{bmatrix} 1 & e^{-j2\pi\frac{d}{\lambda}\sin(\theta_{l,i}+\Delta_i)} & \dots & e^{-j2\pi\frac{d}{\lambda}(N-1)\sin(\theta_{l,i}+\Delta_i)} \end{bmatrix}^T \quad (5.28)$$

where d is the element spacing and $\theta_{l,i}$ is the AOA of the l th path from i th user and Δ_i is the angle spread of the i th user. In the analysis, we will use the narrowband assumption for array processing which states that the envelope of the plane wave propagating across the array remains essentially constant if the bandwidth of either the signal or the antenna is small compared to the carrier frequency. For the wideband case, this assumption is also valid provided that the time taken by the wavefront to pass across the array is small compared to the chip period T_c . Equation (5.28) can be arranged as

$$h_i(t) = \sum_{l=1}^{L_i} a_{l,i}(t) \delta(t - \tau_{l,i}) \quad (5.29)$$

where $a_{l,i}(t) = \alpha_{l,i}(t) a(\theta_{l,i})$ is called the spatial signature vector or the channel vector of the i th user.

5.7 Diversity Techniques in Spatial Channel Models

In the previous sections of this chapter, a detailed mathematical description of the spatio-channel models was presented. In this section, we quantify the performance by simulating the receivers in the GBSB circular and elliptical channels. The performance of receivers for these channels are compared for different diversity combining techniques applied and for varying number of antenna elements used. BER versus E_b/N_0 is considered both for diversity combining techniques as well as for number of antenna elements used.

5.8 Results and Discussion

The assumptions and the iterative steps followed for the simulation process has already been mentioned in chapter 4. The simulation results are mentioned below. In this section we quantify the performance by simulating the receivers in the GBSB circular and elliptical channels. The performances of receivers for these channels are compared for different diversity combining techniques applied and for varying number of antenna elements used. BER versus E_b/N_0 is considered both for diversity combining techniques as well as for number of antenna elements used.

- The performance comparison of the BER values of different diversity combining techniques for varying number of antenna elements for GBSB Circular model is summarized in Table 5.1. The probability of error improves with increase in antenna

elements and MRC gives the best performance level as compared to other diversity combining techniques.

- Table 5.2 compares the BER values of GBSB Elliptical of different diversity combining techniques for varying number of antenna elements used as a function of E_b/N_0 . The performance improves with increase in antenna elements and MRC gives the best performance level as compared to other diversity combining techniques.
- Figure 5.4 and Figure 5.5 describes the performance of 1-path GBSB Elliptical and GBSB Circular Channel Models, respectively. Both the figures show that the probability of error decreases with the increase in the SNR.
- Figure 5.6 shows the variations in the BER for different antenna elements used for GBSB Elliptical Channel model for applied EGC at the receiver. By analyzing the performance level for the use of 2,3,and 4 antennas at the handsets from the figure, it can be easily concluded that the probability of error decreases with the increase in the number of antenna elements.
- Figure 5.7 shows the variations of BER for different antenna elements used for applied Selective Maximum Diversity Combining at the receiver. The performance comparison can easily be made from the figure, which shows that the BER decreases with increase in the number of antenna elements. The figure depicts that the performance improves with the increase in the number of elements and with increasing SNR.
- Figure 5.8 shows the variations of BER for different antenna elements used for applied Maximal Ratio Diversity Combining at the receiver. Following the trend in the curve, it can be inferred from figure 5.8 that BER decreases with increase in number of antenna elements and hence the performance of the antenna system improves. By comparing the results obtained from the three diversity combining techniques it can also be inferred that MRC shows the best performance level as compared to other two diversity combining techniques.
- Figure 5.9 shows the variations in the BER for different antenna elements used for GBSB Circular Channel model for applied Equal Gain Diversity Combining at the receiver. It follows the same trend of increase in performance level with the increase in number of antenna elements.
- The variations in the BER for different antenna elements used for GBSB Circular Channel model for applied Selective Maximum Diversity Combining at the receiver

is shown in Figure 5.10. The performance improves with the increase in the number of antenna elements.

- Figure 5.11 shows the variations in the BER for different antenna elements used for GBSB Circular Channel model for applied Maximal Ratio Diversity Combining at the receiver. By increasing the number of antenna elements, the BER reduces. From figures 5.9 to 5.11, it can be concluded that the BER decreases with the increase in the number of antenna elements used as well as with SNR i.e. the performance increases by increasing the antenna elements at the receiver. Also among the three diversity-combining techniques applied, MRC shows the best results.

Table 5.1 Comparison of BER for GBSB Circular Channel for different no. of antenna elements

No. of Antenna Elements	SNR (dB)	Bit Error Rate		
		EGC	MRC	SMC
2	1	0.0610	0.0605	0.0611
	5	0.0104	0.0103	0.0105
	10	0.0001	0.0001	0.0001

3	1	0.0325	0.0322	0.0373
	5	0.0033	0.0030	0.0036
	10	0.0000	0.0000	0.0000
4	1	0.0181	0.0179	0.0255
	5	0.0010	0.0010	0.0018
	10	0.0000	0.0000	0.0000

Table 5.2 Comparison of BER for GBSB Elliptical Channel for different no. of antenna elements

No. of Antenna Elements	SNR (dB)	Bit Error Rate		
		EGC	MRC	SMC
2	1	0.0992	0.0976	0.0997
	5	0.0453	0.0469	0.0457
	10	0.0085	0.0085	0.0085

3	1	0.0737	0.0717	0.0789
	5	0.0285	0.0280	0.0311
	10	0.0032	0.0028	0.0038
4	1	0.0571	0.0555	0.0677
	5	0.0182	0.0180	0.0242
	10	0.0012	0.0009	0.0023

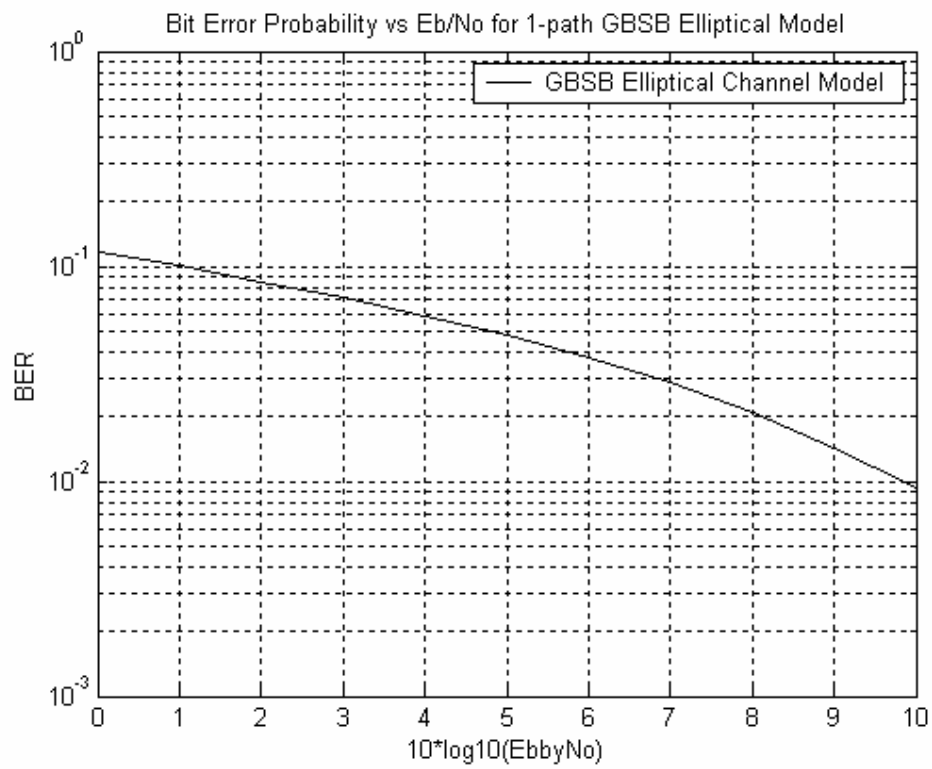


Fig. 5.4 Plot of BER vs. Eb/No for 1-path GBSB Elliptical Channel

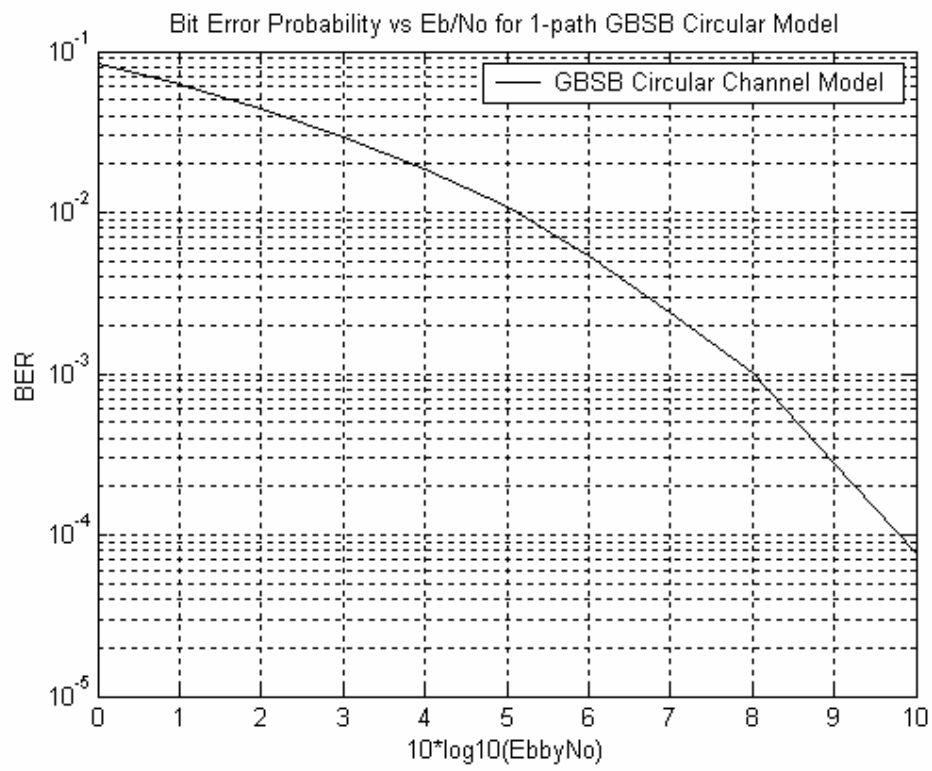


Fig. 5.5 Plot of BER vs. Eb/No for 1-path GBSB Circular Channel

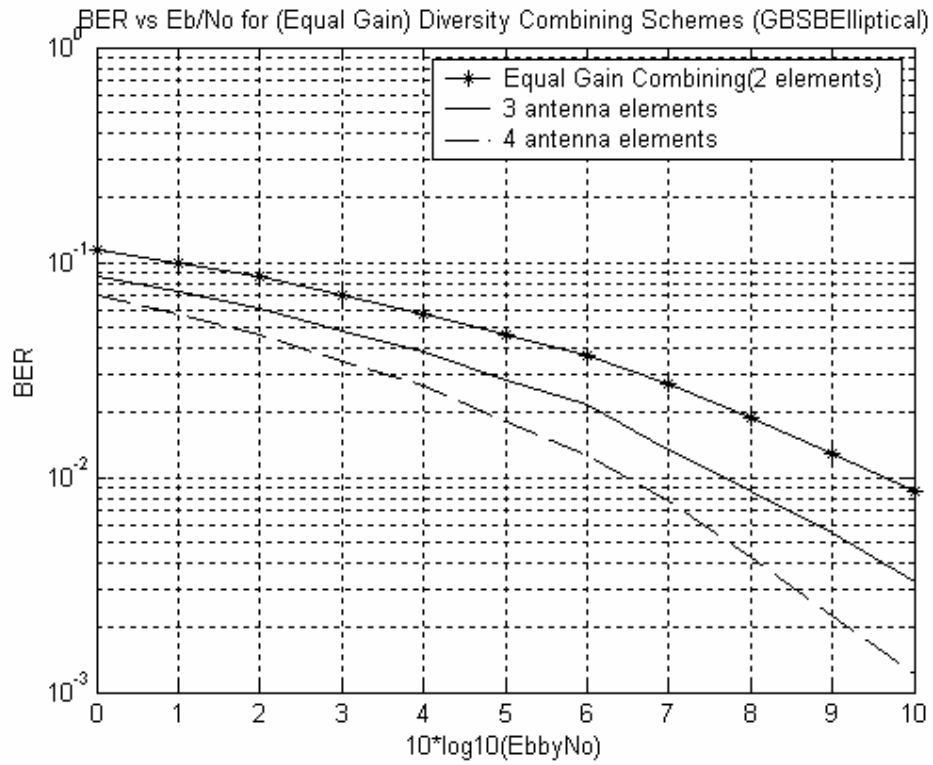


Fig. 5.6 Plot of BER vs. E_b/N_0 for GBSB Elliptical Channel with the increase in the no. of antenna elements using EGC

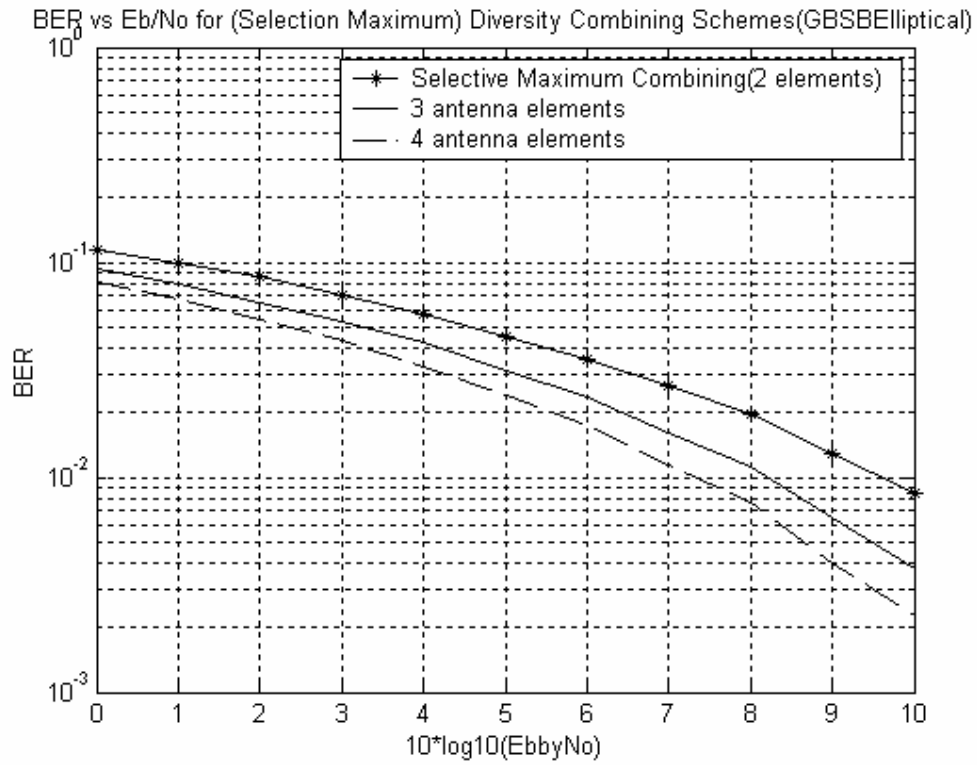


Fig. 5.7 Plot of BER vs. Eb/No for GBSB Elliptical Channel with the increase in the no. of antenna elements using SMC

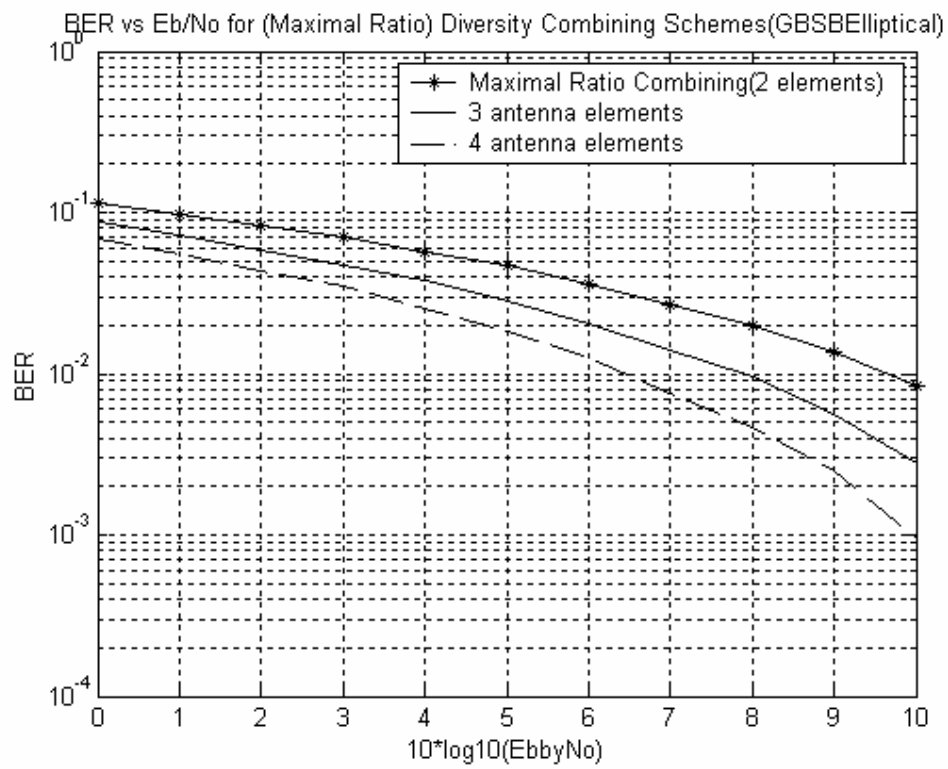


Fig. 5.8 Plot of BER vs. Eb/No for GBSB Elliptical Channel with the increase in the no. of antenna elements using MRC

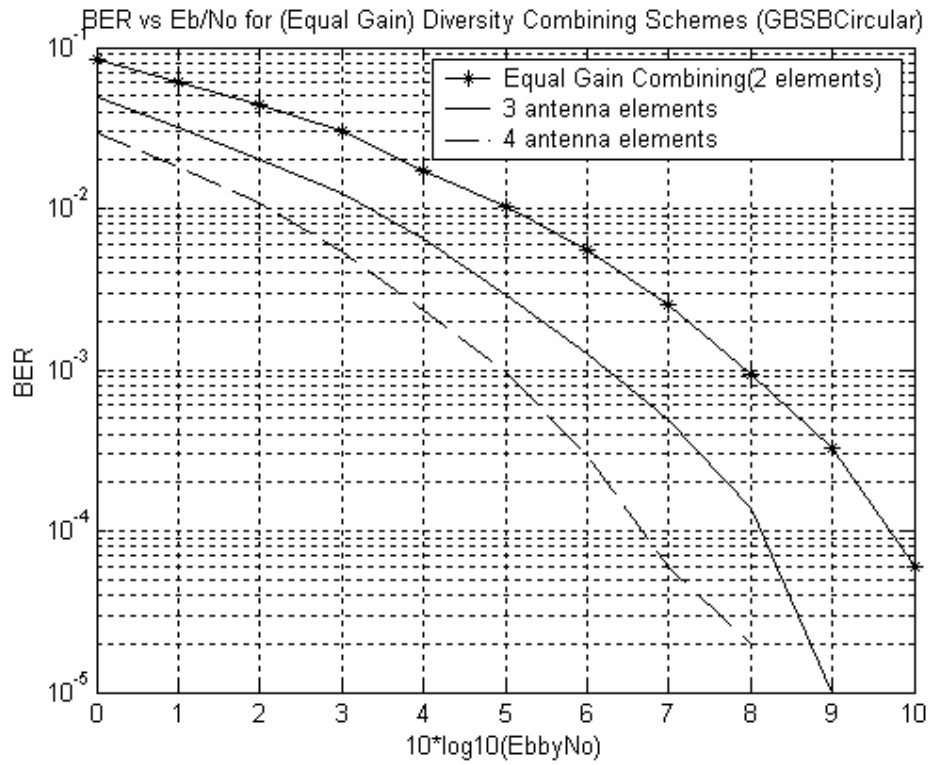


Fig. 5.9 Plot of BER vs. Eb/No for GBSB Circular Channel with the increase in the no. of antenna elements using EGC

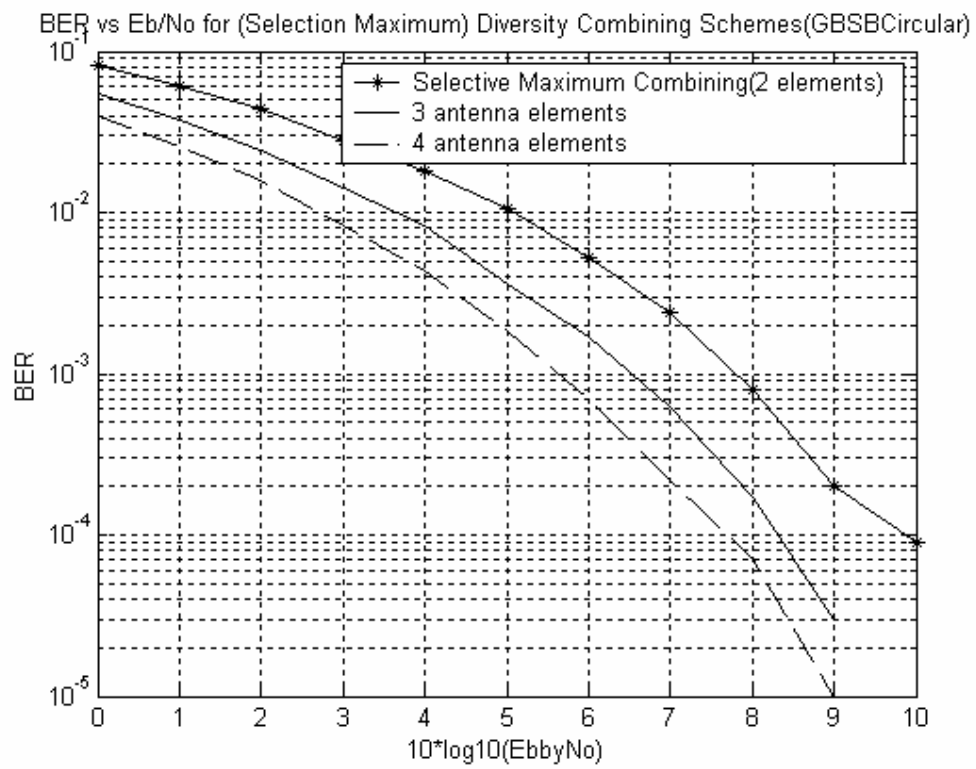


Fig. 5.10 Plot of BER vs. Eb/No for GBSB Circular Channel with the increase in the no. of antenna elements using SMC

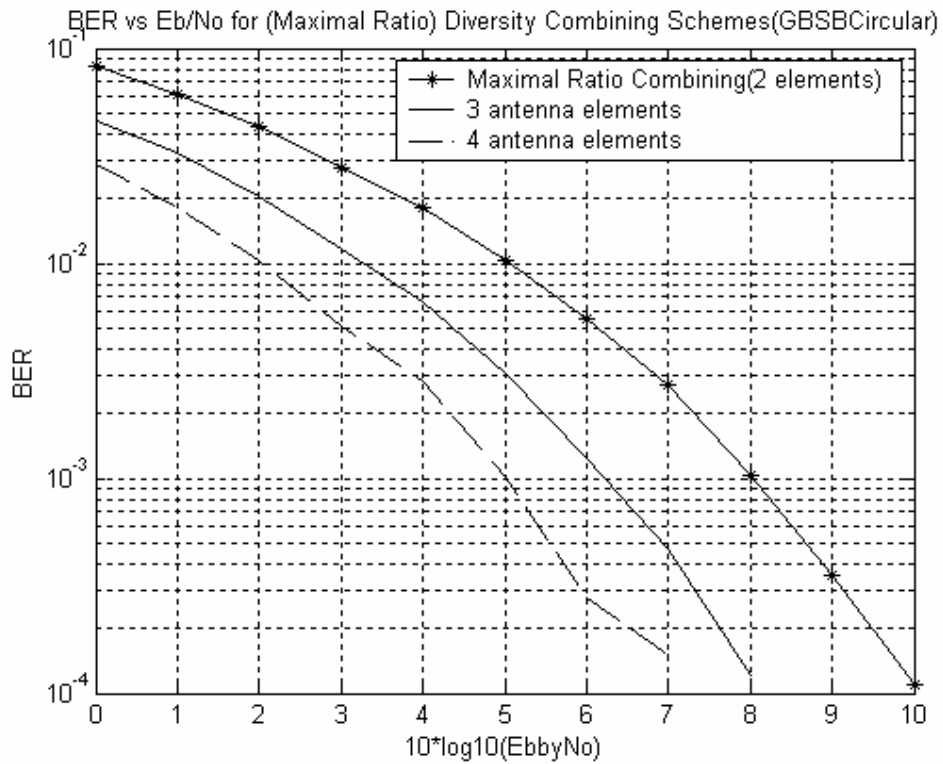


Fig. 5.11 Plot of BER vs. E_b/N_0 for GBSB Circular Channel with the increase in the no. of antenna elements using MRC

Chapter-6 Conclusions and Future Scope

In this dissertation, we propose a smart antenna system incorporated into handsets. The project involves simulation of diversity techniques. Various diversity techniques were simulated in MATLAB. These included Selection Combining (SC), Equal Gain Combining

(EGC), and Maximum Ratio Combining (MRC). The results were used to plot outage probability for various fading channels. The results were compared with closed form analytical expressions and found to be in conformance. The generality and computational efficiency of the simulations make them a powerful means for testing theoretical results and diversity applications. The results detailed in chapter 7 indicate that MRC shows the best performance level among all the diversity combining techniques when applied to various communication channels on the dual smart antenna systems. Also, simulations carried out for varying number of antenna elements show that the performance of the antenna system improves as the number of antenna elements increase. However even in this case MRC shows the best performance i.e. the BER improves with the increase in the SNR. Hence it can be finally concluded that EGC receiver performance is superior to selection diversity performance while it is only marginally inferior as compared to MRC. EGC is often used in practice because of its reduced complexity relative to the optimum MRC scheme. This is because the latter requires the knowledge of the fading amplitude in each signal branch while the former requires no such knowledge

In future these diversity techniques can further be applied to the more realistic frequency-selective fading channel models. Moreover, the work can also be extended to other combining techniques like Optimum Combining and Adaptive Combining.

References

- [1] Christodoulou C. and Herscovici N., ‘Smart Antennas in Wireless Communications: Base-Station Diversity and Handset Beamforming’, IEEE Antennas and Propagation Magazine Vol.3 (5), pp.142-151, 2000
- [2] Malika Greene, “Radiocommunication Agency”, Public Wireless System, June 2002
- [3] Howard Bonds III, System Performance in Fading Channel Environments, M.S.E.E, May 2003

- [4] Winter, J, “ Adaptive Antenna arrays for wireless systems,” Tutorial at IEEE 49th Vehicular Technology Conference, Houston, Texas, 16-20 May, 1999
- [5] Won Kim S., Sam HA D. and Ho Kim J., ‘Performance Gain of Smart Antennas with diversity combining at handsets for the 3GPP WCDMA system, 2000.
- [6] Dietrich Jr., CB, “Adaptive Arrays and Diversity Antenna Configurations for handheld wireless Communication Terminals”, Dissertation, Virginia Polytechnic Institute and State University, Blacksburg, Virginia, 15 February 2000
- [7] M. K. Simon and M. S. Alouini, “A unified approach to performance analysis of digital communications over fading channels,” *Proc. IEEE*, Vol. 86, pp. 1860-1877, Sep. 1998.
- [8] A. Annamalai, V. Ramanathan and C. Tellambura, “Analysis of Equal Gain Diversity Receiver in Correlated Fading Channels,” *Proc. IEEE Vehicular Technology Conference*, Vol. 4, pp. 2038-2041, Fall 2002.
- [9] P. Lombardo, F. Fedele, M. M. Rao, “MRC Performance for Binary Signals in Nakagami Fading with General Branch Correlation”, *IEEE Transactions on Communications*, Vol. 47, No. 1, pp.44-50, January 1999.
- [10] A.M.D. Turkmani, A.A. Arowogolu, P.A. Jefford, and C.J. Kellent, “An Experimental Evaluation of Performance of Two-Branch Space and Polarization Diversity Schemes at 1800 MHz,” *IEEE Trans. Veh. Tech.*, vol. 44, no.2, pp. 318-326, May 1995.
- [11] Seedahmed S. Mahmoud, Zahir M. Hussain, and Peter O’Sheay, “Space-Time Geometrical-Based Channel Models: A Comparative Study”
- [12] J. C. Liberti, T. S. Rappaport, “A Geometrically Based Model for Line-of-Sight Multipath Radio Channels,” *IEEE Vehicular Technology Conference*, Atlanta, GA, April 29-May1, 1996.
- [13] P. Petrus, J. H. Reed, and T. S. Rappaport, “Geometrically based statistical channel model for macro cellular mobile environments,” in *Proc., IEEE Veh. Tech. Conf.*, pp. 844-848, Apr. 1996.
- [14] Theodore S. Rappaport, “Wireless Communications, Principles and practices”, Second Edition
- [15] William C. Y. Lee, “Mobile Communications Engineering, theory and applications”, Second edition
- [16] Vijay K. Garg, Joseph E. Wilkes, “Wireless and personal communications systems”,
- [17] “Maximal Ratio Combining with Correlated Rayleigh Fading Channels”, EE359: Wireless Communications, December 7, 2002
- [18] Daniel S. Baum, “Simulating the SUI Channel Models”, Stanford University, IEEE 802.16.3c-01/53

- [19] Jianxia Luo, James R. Zeidler, "A Statistical Simulation Model for Correlated Nakagami Fading Channels", Electrical and Computer Engineering Department, University of California, San Diego, 9500 Gilman Drive, La Jolla, CA 92093-0407 USA
- [20] J. Eric Nuckols, "Implementation of Geometrically Based Single- Bounce Models for simulation of Angle-of-Arrival of Multipath Delay Components in the Wireless Channel Simulation Tools, SMRCIM and SIRCIM", Virginia Polytechnic Institute and State University, Dec 1999.
- [21] R.B. Ertel, P. Cardieri, K.W. Sowerby, T.S. Rappaport, and J.H. Reed, "Overview of Spatial Channel Models for Antenna Array Communication Systems," IEEE Personal Communications, Vol. 5, No. 1, February 1998.
- [22] J. C. Liberti, T. S. Rappaport, "A Geometrically Based Model for Line-of-Sight Multipath Radio Channels," IEEE Vehicular Technology Conference, Atlanta, GA, April 29-May1, 1996.